ISSN 2096-7071 (Print)
ISSN 2096-3101 (Online)
CN 10-1629/R1

CHINA CDC WEEKLY

Vol. 6 No. 41 Oct. 11, 2024

中国疾病预防控制中心周报

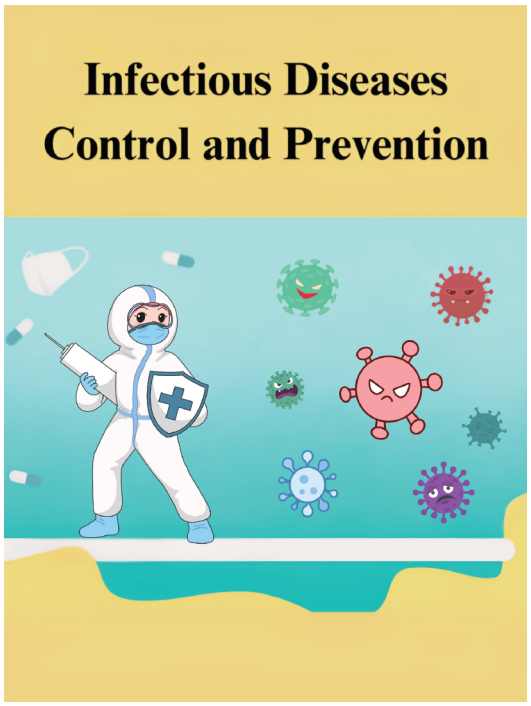

INFECTIOUSE DISEASE ISSUE

ISSN 2096-7071
9 772096 707248 41>

China CDC Weekly

Cover Image: adapted from Canva, https://www.canva.cn/.

Vital Surveillances

Epidemiological Characteristics of Dengue Fever — China, 2005–2023

Zhuowei Li[1]; Xiaoxia Huang[1]; Aqian Li[1]; Shanshan Du[1]; Guangxue He[1]; Jiandong Li[1,#]

ABSTRACT

Introduction: The global incidence of dengue fever has increased significantly over the past two decades, and China faces a significant upward trend in dengue control challenges.

Methods: Data were obtained from China's NNDRS from 2005 to 2023. Joinpoint regression software was used to analyze temporal trends, while SaTScan software was used to analyze spatial, seasonal, and spatiotemporal distributions. ArcGIS software was used to visualize clusters.

Results: A total of 117,892 dengue cases were reported from 2005 to 2023, with significant fluctuation in annual reported cases. Dengue was not endemic in China. Autochthonous outbreaks most likely occurred in the southwestern, southeastern coastal, and inland areas of China. These outbreaks have occurred between June and November, generally peaking in September or October, around epidemiological week (EW) 40.

Conclusions: Dengue challenges in China are increasing. Timely case monitoring, proactive control interventions, and staff mobilization should be implemented before June to ensure a timely response to autochthonous outbreaks.

Dengue virus (DENV) is the most widespread arbovirus and causes the highest number of arboviral disease cases globally. DENV contains four serotypes (DENV-1, DENV-2, DENV-3, and DENV-4). Infection with one serotype can induce only transient immunity to the others; secondary infections with a different serotype may increase the risk of severe dengue (*1*–*3*). Over the past two decades, the global incidence of dengue has increased markedly (*4*), and the challenges of dengue outbreaks faced by China have also shown a cyclical upward trend (*5*). Since the first confirmed autochthonous outbreak of dengue was reported in Guangdong Province in 1978, outbreaks caused by all four DENV serotypes have been reported successively on a fluctuating scale in China (*5*). In January 2024, several Member States from the World Health Organization (WHO) Regions of the Americas, Africa, Western Pacific, and Southeastern Asia reported a significant increase in dengue circulation (*6*). Travel-related cases may always occur in areas with the potential for rapid dengue transmission, posing an increasing risk of autochthonous outbreaks in China.

To better understand the dengue epidemic in China, we analyzed the epidemiological characteristics of reported dengue cases in China from 2005 to 2023. We examined temporal, spatial, and population characteristics, as well as clustering patterns.

METHODS

Data Collection

Dengue case data for China from January 1, 2005, to December 31, 2023, were obtained from the Chinese National Notifiable Disease Reporting System (NNDRS). Demographic data stratified by age and sex were obtained from the National Bureau of Statistics of China (https://www.stats.gov.cn/sj/tjgb/rkpcgb/, accessed on January 5, 2024).

Descriptive Analysis

Descriptive epidemiologic methods were used to analyze the reported cases. Joinpoint regression software was used to analyze temporal trends of dengue cases. Incidence was analyzed by spatial, space-time, and seasonal scanning with SaTScan (version 10.1.2; Information Management Services, Maryland, USA) software at the prefecture and month levels, respectively. Datasets were prepared based on incidence, population by district, and geographic coordinates. The maximum scanning window was set to 25% of the total population. The maximum temporal clustering scale was set to 50% of the total study length, and the step size was set to 1 month, as

described previously (*7*). Dengue clusters were identified using a model based on the maximum log-likelihood ratio (LLR) and graded by log-likelihood values. A cluster of dengue cases in the selected region was accepted when $P \leq 0.05$. Areas under risk were calculated by comparing the number of cases within each window to the expected number using a Poisson model. Relative risk (*RR*) in the SaTScan output file refers to the ratio of estimated risks within and outside the cluster. Areas at risk of infection were determined by the *RR*.

RESULTS

From 2005 to 2023, a total of 117,892 cases were reported in China. Of these, 67,073 (56.89%) were laboratory-confirmed cases, and 3,225 (2.74%) were imported cases. The national incidence of dengue significantly increased from 2005 to 2023 (AAPC=30.27%, 95% *CI*: 21.44, 159.66%) with an average incidence rate of 0.45/100,000. The number of reported cases peaked in 2014 (47,047 cases), 2019 (22,726 cases), and 2023 (19,935 cases), accounting for approximately 76.09% of total reported cases (Figure 1A). The number of annual reported cases fluctuated significantly, ranging from 59 cases (2005) to 47,047 cases (2014), and exhibited three successive phases (Figure 1A). A low-incidence phase was observed during 2005–2012, with an average incidence rate of 0.03/100,000 (AAPC=−10.54%, 95% *CI*: −30.84, 10.80%). A high-incidence phase was observed during 2013–2019, with an average incidence rate of 0.96/100,000 (AAPC=−13.25%, 95% *CI*: −40.26, 16.68%). A significant decline in cases, with an average incidence rate of 0.03/100,000 (AAPC=−14.88%, 95% *CI*: −58.37, 59.20%), was seen during the COVID-19 pandemic from 2020 to 2022. In 2023, the number of cases approached the 2019 peak, continuing the characteristics of the high-incidence phase.

Dengue was reported in all months; however, the vast majority of cases were reported from June to November. The peak occurred from August to October (*n*=101,653, *RR*=18.60, LLR=97,644.65), accounting for 86.23% of the total (Figure 1B). When analyzed by epidemiological week (EW) of onset or reporting, the number of cases generally peaked at EW 40 (*n*=15,166, Figure 1C). In low-incidence years, the peak could appear later, such as in EW 43 in 2012.

The overall male-to-female case ratio was 1.11. A relatively similar age distribution was observed for both males and females (Figure 2A). Cases were reported in all age groups; the majority (*n*=68,698; 58.27%) were 20–49 years of age (Figure 2B). The main difference in

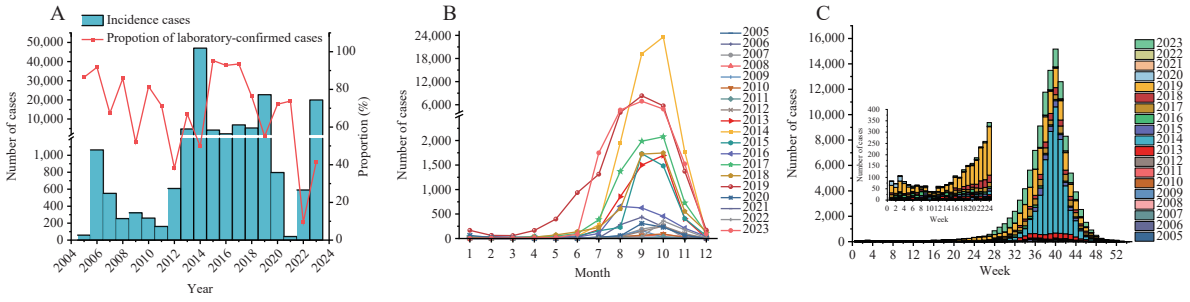

FIGURE 1. Distribution of dengue cases in the Chinese mainland during 2005–2023. (A) By year; (B) By month; (C) By week.

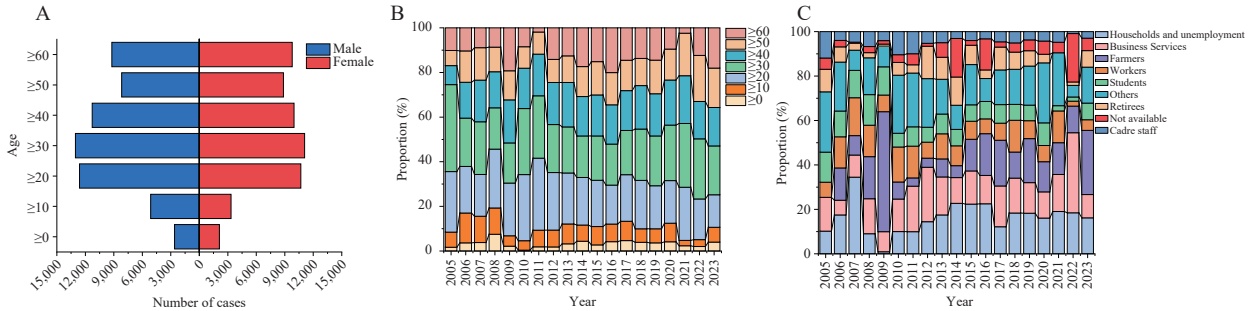

FIGURE 2. Distribution of dengue by (A) gender, (B) age, and (C) occupation.

the sex ratio was that the proportion of females was lower than that of males of the same age in the 50–59 (0.92∶1) and 60 and above age groups (0.94∶1), while the opposite was true for the 0–9 (1.24∶1), 10–19 (1.53∶1), 20–29 (1.18∶1), 30–39 (1.18∶1), and 40–49 (1.13∶1) age groups. The highest incidence of cases was observed among households and unemployed individuals (*n*=22,943, 19.46%), followed by farmers (*n*=16,901, 14.34%) and businesspeople (*n*=15,258, 12.94%) (Figure 2C).

From 2005 to 2023, dengue was reported in 30 provincial-level administrative divisions (PLADs), including 302 prefectures and 1,694 counties. The top five PLADs with high dengue incidence — Guangdong (68,070, 57.74%), Yunnan (30,785, 26.11%), Fujian (3,742, 3.17%), Zhejiang (3,260, 2.77%), and Guangxi (3,136, 2.66%) — contributed 92.45% of the total cases. Additionally, 68.34% of cases were reported from the top five prefectures: Guangzhou (45,977, 39.00%), Xishuangbanna (15,871, 13.46%), Dehong (10,073, 8.54%), Foshan (5,998, 5.09%), and Zhongshan (2,652, 2.25%). The top five counties — Baiyun (13,303, 11.28%), Jinghong (11,171, 9.48%), Ruili (9,210, 7.81%), Haizhu (6,899, 5.85%), and Liwan (6,680, 5.67%) — accounted for 40.09% of cases. Dengue exhibited obvious geographical clustering in the Chinese mainland.

During the low-incidence phase from 2005 to 2012, clusters occurred mainly in Guangdong (11 prefectures, *n*=2,217), Yunnan (3 prefectures, *n*=181), Fujian (1 prefecture, *n*=142), and Zhejiang (1 prefecture, *n*=201). During the high-incidence phase, the geographic scope of clusters expanded, and autochthonous outbreaks occurred in the southwestern, southeastern coastal, and inland areas of Chinese mainland. This was especially true in the Pearl River Delta (PRD) and the Border of Yunnan and Myanmar (BYM), with cases reported in Guangdong (10 prefectures, *n*=62,375), Yunnan (7 prefectures, *n*=29,578), Fujian (1 prefecture, *n*=1,831), Zhejiang (1 prefecture, *n*=1,583), Jiangxi (1 prefecture, *n*=833), and Guangxi (1 prefecture, *n*=1,842).

The spatiotemporal analysis of incidence, population, and geographic coordinates from 2005 to 2023 identified significant dengue clusters categorized into three levels. The primary cluster emerged in Guangzhou (*n*=37,382) and Foshan (*n*=3,543) in Guangdong Province in 2014 (*RR*: 589.08, LLR: 210,880.11), and in seven prefectures in southwestern Yunnan Province (*n*=27,689) (Xishuangbanna, Pu'er, Lincang, Dehong, Dali, Chuxiong, Baoshan) from 2015 to 2023 (*RR*: 56.27, LLR: 80,673.22). Secondary clusters (*n*=5,387) were identified in southeastern prefectures of Zhejiang (11 prefectures), Anhui (5 prefectures), Fujian (9 prefectures), Jiangxi (10 prefectures), and Guangdong (4 prefectures) in 2019 (*RR*: 7.05, LLR: 5,807.61), and in Chongqing Municipality (*n*=1,411) in 2019 (*RR*: 9.95, LLR: 1,965.70). Tertiary clusters were found in Puyang (*n*=90), Henan Province (*RR*: 5.34, LLR: 77.56) in 2019, and Jining (*n*=81), Shandong Province (*RR*: 2.16, LLR: 18.92) in 2017. The frequency of high-risk areas suggests that dengue is not endemic in China; however, widespread areas are vulnerable to autochthonous outbreaks.

CONCLUSIONS

Dengue affects people in most countries in the tropics and subtropics. Dengue is not endemic in the Chinese mainland; however, the vectors that transmit DENV are widely distributed. *Aedes aegypti* is established notably in parts of Yunnan, Hainan, and Guangdong, and *Aedes albopictus* is widely established in much of China (*5*). In this study, the spatial, temporal, and demographic epidemiological characteristics of dengue, as well as the areas with local transmission risks, were revealed in China from 2005 to 2023. No significant gender or occupational differences were observed in the reported cases. It could be supposed that susceptibility to dengue might mainly depend on the proximity to the source of infection and the chance of being bitten by infected mosquitoes in China. The likelihood of onward DENV transmission is linked to the importation of the virus into receptive areas with active, competent vectors (*6*,*8*). Globally increased dengue circulation over the past two decades has markedly increased the risk of importation of the virus by viremic travelers into China. All autochthonous outbreaks of dengue in China have so far occurred between June and November, generally peaking in September or October, around EW 40. The spatial and spatiotemporal distribution of dengue in the past 19 years demonstrated that broad areas in China are facing the risk of autochthonous outbreaks, which most likely occur in the southwestern, southeastern coastal, and inland areas of south China, especially in the areas of the PRD and BYM. Most PLADs in South China have reported locally acquired dengue cases.

Factors contributing to local transmission include

high mosquito populations, susceptibility to circulating DENV serotypes, and favorable environmental conditions — such as air temperature, precipitation, and humidity — that affect mosquito reproduction, feeding patterns, and the DENV incubation period (*9*–*11*). Timely, proactive control interventions and qualified staff are also key influencing factors. Proactive prevention and control interventions should be deployed, and staff training and mobilization should be carried out before June for timely responses to autochthonous outbreaks in the Chinese mainland.

This study is based on the analysis of online active reporting data from the NNDRS system, which, to some extent, affects the accurate portrayal of dynamic dengue epidemic characteristics in specific regions. However, it can reflect the overall dengue trend in China and provide a reference for promoting the proactive deployment of prevention and control.

Conflicts of interest: No conflicts of interest.

Funding: This work was supported by the Project of Capital Clinical Diagnosis and Treatment Technology Research and Transformation (Z221100007422076).

doi: 10.46234/ccdcw2024.217

[#] Corresponding author: Jiandong Li, lijd@ivdc.chinacdc.cn.

[1] National Key Laboratory of Intelligent Tracking and Forecasting for Infectious Diseases, NHC Key Laboratory of Biosafety, NHC Key Laboratory of Medical Virology and Viral Diseases, National Institute for Viral Disease Control and Prevention, Chinese Center for Diseases Control and Prevention, Beijing, China.

Submitted: March 25, 2024; Accepted: May 20, 2024

REFERENCES

1. Guzman MG, Harris E. Dengue. Lancet 2015;385(9966):453 – 65. https://doi.org/10.1016/S0140-6736(14)60572-9.
2. Wilder-Smith A, Ooi EE, Horstick O, Wills B. Dengue. Lancet 2019;393(10169):350 – 63. https://doi.org/10.1016/S0140-6736(18)32560-1.
3. Bhatt S, Gething PW, Brady OJ, Messina JP, Farlow AW, Moyes CL, et al. The global distribution and burden of dengue. Nature 2013;496(7446):504 – 7. https://doi.org/10.1038/nature12060.
4. WHO. Dengue-Global situation. (2024-01-05) [2024-01-05]. https://www.who.int/emergencies/disease-outbreak-news/item/2023-DON498.
5. Yue YJ, Liu QY, Liu XB, Zhao N, Yin WW. Dengue fever in Mainland China, 2005-2020: a descriptive analysis of dengue cases and *Aedes* data. Int J Environ Res Public Health 2022;19(7):3910. https://doi.org/10.3390/ijerph19073910.
6. European Centre for Disease Prevention and Control. Dengue worldwide overview. (2024-03-03) [2024-03-03]. https://www.ecdc.europa.eu/en/dengue-monthly.
7. Liu KK, Sun JM, Liu XB, Li RY, Wang YG, Lu L, et al. Spatiotemporal patterns and determinants of dengue at county level in China from 2005-2017. Int J Infect Dis 2018;77:96 – 104. https://doi.org/10.1016/j.ijid.2018.09.003.
8. Islam MT, Quispe C, Herrera-Bravo J, Sarkar C, Sharma R, Garg N, et al. Production, transmission, pathogenesis, and control of dengue virus: a literature-based undivided perspective. Biomed Res Int 2021;2021:4224816. https://doi.org/10.1155/2021/4224816.
9. WHO. Dengue and severe dengue. (2024-03-03) [2024-03- 03]. https://www.who.int/zh/news-room/fact-sheets/detail/dengueand-severe-dengue.
10. Bashir A. How climate change is changing dengue fever. BMJ 2023;382:1690. https://doi.org/10.1136/bmj.p1690.
11. Liu HM, Huang XD, Guo XX, Cheng P, Wang HF, Liu LJ, et al. Climate change and *Aedes albopictus* risks in China: current impact and future projection. Infect Dis Poverty 2023;12(1):26. https://doi.org/10.1186/s40249-023-01083-2.

Vital Surveillances

Trends and Spatial Pattern Analysis of Typhoid and Paratyphoid Fever Incidence — Yunnan Province, China, 1989–2022

Xiulian Shen[1,&]; Liqiong Zhang[2,&]; Lining Guo[3]; Jibo He[1,#]; Weijun Yu[4,#]

ABSTRACT

Introduction: This study explored the incidence trends and spatial clustering of typhoid and paratyphoid fever (TPF) in Yunnan Province to provide scientific evidence for developing and improving prevention and control strategies.

Methods: Temporal trends were investigated by calculating the annual percent change (APC) and average annual percent change (AAPC), along with their 95% confidence intervals (*CI*s). The spatial clustering of TPF across Yunnan Province was examined using global Moran's I and local indicators of spatial association (LISA) statistics.

Results: A total of 206,066 TPF cases were reported in Yunnan Province from 1989 to 2022, with an average annual incidence of 13.98 per 100,000 population and a case fatality rate of 2.5 per 1,000. The greatest number of cases was reported during July and August. The 25–34-year age group had the highest incidence, and farmers were prominently represented. TPF incidence in Yunnan Province showed a significant decrease and spatial clustering. From 2005 to 2022, 13 county-level cities/counties/municipal districts in 5 prefectures (cities) in Yunnan Province were identified as statistically significant H-H spatial clusters of TPF incidence. A total of 24 TPF outbreaks were reported in Yunnan Province from 2005 to 2022.

Conclusions: The incidence of TPF in Yunnan Province showed a significant decrease and spatial clustering. Control strategies should focus on high-incidence areas, seasons, and populations to reduce the incidence of TPF.

Typhoid and paratyphoid fever (TPF) are categorized as Class B notifiable infectious diseases in China. They are caused by the *Salmonella enterica* subspecies serovars Typhi and Paratyphi A, B, and C. TPF is characterized by a predominantly gastrointestinal reaction, high infectiousness, long duration of illness, multiple complications, and a substantial disease burden. The global incidence of TPF has declined, with approximately 14.3 million cases and 135,900 deaths reported in 2017 (*1*). Since the 1990s, the incidence of TPF in China has declined annually and is at a low level according to World Health Organization classification criteria (*2*). However, the incidence of TPF in southwestern PLADs, such as Yunnan Province, is among the highest in the country and remains a priority infectious disease for prevention and control (*2*). Therefore, understanding the epidemiological trends of TPF and analyzing population and regional distribution characteristics is important for devising effective control plans, strategies, and interventions. Herein, these topics were examined using TPF data collected from 1989 to 2022. Descriptive, temporal trend, and spatial autocorrelation analyses were performed.

METHODS

Data on TPF for 1989–2004 were obtained from the Compendium of Infectious Disease Epidemics in Yunnan Province. Reported TPF cases for 2005–2022 were obtained from the infectious disease surveillance system of the CISDCP (*3*). Additionally, reported TPF outbreaks for 2005–2022 were obtained from the emergent public health event information management system of the CISDCP. Outbreak definitions followed the National Public Health Emergency Information Reporting and Management Specification issued by the Ministry of Health of the People's Republic of China in 2005 (*4*). Demographic data were derived from the Yunnan Statistical Yearbook (1989–2022). Administrative division codes and geographical coordinates were acquired from the National Catalogue Service for Geographic Information (https://www.webmap.cn/). The crude incidence rate (per 100,000 population) was calculated as the number of annual TPF cases divided by the total annual

population.

Joinpoint regression models were employed to identify incidence trends from 1989 to 2022 using Joinpoint software (version 4.9.1.0; National Cancer Institute, Bethesda, US) (*5*). The number of joinpoints, joinpoint locations, and *P* values were determined using Monte Carlo permutation tests. The Bayesian information criterion was used to select the best-fitting model. To explore temporal trends, the APC and AAPC in reported TPF cases and their 95% confidence intervals (*CI*s) were calculated. An increasing or decreasing trend indicates a statistically significant trend slope (two-sided $P<0.05$). A stable trend indicates a non-significant APC (two-sided $P\geq 0.05$), representing stable incidence or sporadic case reporting (*6*).

Spatial autocorrelation analysis, using GeoDa 1.18.0.0, explored the spatial correlation strength of TPF. Details on the spatial autocorrelation analysis have been previously published (*3*). Briefly, global autocorrelation, using Global Moran's I statistics, analyzed the clustering characteristics of the research objects across the entire region. Anselin's Local Moran's I (LISA) test statistics were used for spatial autocorrelation analysis. LISA analyzed the specific cluster types and regions; LISA cluster maps showed four cluster modes: H-H, L-L, L-H, H-L, and not significant. The H-H and L-L regions represent spatial clustering, while the L-H and H-L regions were outliers (*3*,*7*).

RESULTS

General Characteristics

From 1989 to 2022, Yunnan Province reported 206,066 TPF cases, with an incidence of 32.80 per 100,000 in 1989 and 2.29 per 100,000 in 2022. The average annual incidence was 13.98 per 100,000. A total of 508 deaths were reported, resulting in a case fatality rate of 2.5 per 1,000. Joinpoint regression analysis revealed an overall decreasing trend in TPF incidence, with an AAPC of –6.78% ($P<0.05$) (Figure 1).

From 2005 to 2022, a total of 75,747 TPF cases were reported in Yunnan Province, including 43,767 laboratory-confirmed cases and 31,980 clinically diagnosed cases. Of these, 48,452 had typhoid fever, with incidence decreasing from 14.44 per 100,000 population in 2005 to 1.88 per 100,000 in 2022. The remaining 27,295 cases had paratyphoid fever, with incidence decreasing from 8.24 per 100,000 population in 2005 to 0.41 per 100,000 in 2022. Additionally, joinpoint regression analysis revealed an overall decreasing trend in both typhoid and paratyphoid fever incidence from 2005 to 2022, with average annual percent changes (AAPCs) of –12.51% and –16.79%, respectively (all $P<0.05$) (Figure 2).

Population and Seasonal Distribution

From 2000 to 2022, Yunnan Province reported 112,160 TPF cases, with an incidence rate of 20.13 per 100,000 in females and 19.58 per 100,000 in males. Incidence was elevated in the 0–44 age group, peaking in the 25–34 age group (Table 1). From 2005 to 2022, the primary occupations of TPF cases were farmers, students, and children, comprising 44.01%, 19.08%, and 11.35% of cases, respectively. TPF cases were consistently reported from January to December each year, demonstrating clear seasonality. Peak incidence occurred in July and August (Supplementary Figure S1, available at https://weekly.chinacdc.cn/).

Spatial Distribution

From 1989 to 2022, TPF cases were reported in 8

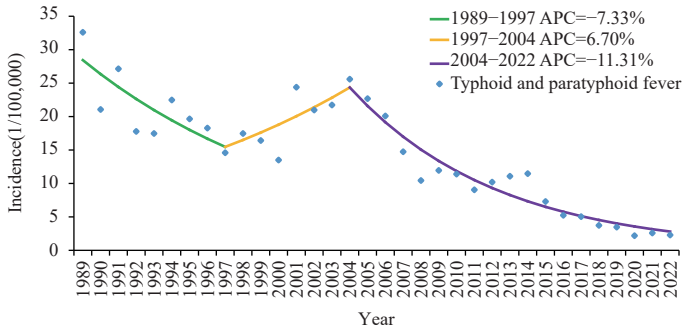

FIGURE 1. Joinpoint regression showing trends in the overall incidence of typhoid and paratyphoid fever in Yunnan Province, China, 1989–2022.

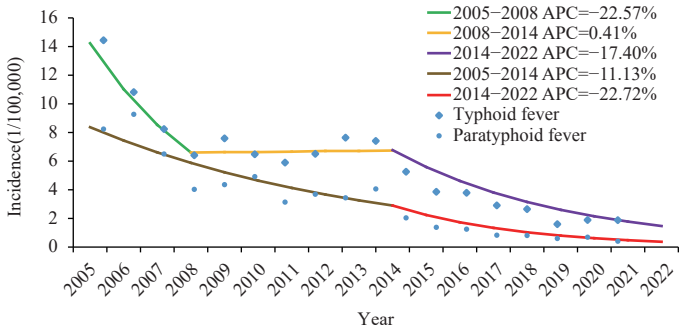

FIGURE 2. Joinpoint regression showing trends in the overall incidence of typhoid fever and paratyphoid fever in Yunnan Province, China, 2005–2022.
Abbreviation: APC=annual percent change.

TABLE 1. Age and gender characteristics of typhoid and paratyphoid fever cases in Yunnan Province, China, 2000–2022.

Age (years)	Total			Male			Female		
	Cases (*n*)	Percentage (%)	Incidence (per 100,000)	Cases (*n*)	Percentage (%)	Incidence (per 100,000)	Cases (*n*)	Percentage (%)	Incidence (per 100,000)
0–4	7,518	6.70	10.70	4,276	56.88	11.77	3,242	43.12	9.55
5–9	9,536	8.50	12.88	5,282	55.39	13.66	4,254	44.61	12.04
10–14	8,734	7.79	11.47	4,894	56.03	12.23	3,840	43.97	10.64
15–19	10,134	9.04	12.02	5,158	50.90	11.67	4,976	49.10	12.39
20–24	11,022	9.83	12.72	5,225	47.41	11.60	5,797	52.59	13.94
25–29	12,007	10.71	15.59	5,861	48.81	14.51	6,146	51.19	16.78
30–34	11,454	10.21	13.69	5,699	49.76	12.95	5,755	50.24	14.52
35–39	9,991	8.91	11.35	4,944	49.48	10.64	5,047	50.52	12.15
40–44	7,957	7.09	10.00	3,954	49.69	9.45	4,003	50.31	10.61
45–49	6,348	5.66	8.83	3,114	49.05	8.32	3,234	50.95	9.38
50–54	5,121	4.57	9.59	2,428	47.41	8.84	2,693	52.59	10.37
55–59	3,709	3.31	7.84	1,801	48.56	7.50	1,908	51.44	8.19
60–64	2,841	2.53	8.10	1,389	48.89	7.84	1,452	51.11	8.37
65–69	2,087	1.86	7.24	1,104	52.90	7.77	983	47.10	6.72
70–74	1,769	1.58	8.01	954	53.93	9.00	815	46.07	7.10
75–79	1,126	1.00	7.62	696	61.81	10.24	430	38.19	5.38
80–84	559	0.50	6.72	352	62.97	9.89	207	37.03	4.35
≥85	247	0.22	6.68	166	67.21	11.87	81	32.79	3.52
Total	112,160	100.00	19.84	57,297	51.09	19.58	54,863	48.91	20.13

autonomous prefectures and 8 cities in Yunnan Province. In terms of average annual incidence, the top 5 prefectures (cities) were Xishuangbanna Dai Autonomous Prefecture (37.50 per 100,000), Dehong Dai-Jingpo Autonomous Prefecture (28.34 per 100,000), Yuxi City (26.88 per 100,000), Nujiang Lisu Autonomous Prefecture (22.39 per 100,000), and Honghe Hani and Yi Autonomous Prefecture (21.29 per 100,000). Joinpoint regression analysis revealed a statistically significant decreasing trend (all $P<0.05$) in the reported incidence of 13 prefectures (cities) from 1989 to 2022, except for Yuxi City ($P=0.288$), Diqing Tibetan Autonomous Prefecture ($P=0.332$), and Nujiang Lisu Autonomous Prefecture ($P=0.468$) (Table 2). Furthermore, there was a positive spatial correlation and significant spatial clustering distribution of TPF incidence in all county-level cities/counties/municipal districts of Yunnan Province from 2005 to 2010 (Moran's I=0.291, $P=0.001$), 2011 to 2016 (Moran's I=0.269, $P=0.001$), 2017 to 2022 (Moran's I=0.241, $P=0.001$), and 2005 to 2022 (Moran's I=0.315, $P=0.001$). Supplementary

TABLE 2. Joinpoint regression showing the incidence and trends of typhoid and paratyphoid fever in the prefectures (cities) of Yunnan Province, China, 1989–2022.

Prefecture/city	Cases (*n*)	Incidence (per 100,000)	Trend	Average annual percent change (95% *CI*s)	*t*	*P*
Xishuangbanna Dai Autonomous Prefecture	12,722	37.50	Decrease	−8.41 (−13.27, −3.28)	−3.16	0.002
Dehong Dai-Jingpo Autonomous Prefecture	10,745	28.34	Decrease	−8.80 (−15.18, −1.95)	−2.49	0.013
Yuxi City	19,356	26.88	Stable	−7.28 (−19.34, 6.59)	−1.06	0.288
Nujiang Lisu Autonomous Prefecture	3,804	22.39	Stable	−5.17 (−17.83, 9.44)	−0.73	0.468
Honghe Hani and Yi Autonomous Prefecture	30,503	21.29	Decrease	−4.72 (−7.09, −2.30)	−3.77	<0.001
Kunming City	34,463	18.12	Decrease	−6.59 (−8.83, −4.31)	−5.53	<0.001
Wenshan Zhuang and Miao Autonomous Prefecture	17,335	15.07	Decrease	−11.69 (−20.50, −1.91)	−2.32	0.020
Baoshan City	10,826	13.17	Decrease	−12.38 (−16.29, −8.28)	−2.27	0.023
Dali Bai Autonomous Prefecture	11,151	9.78	Decrease	−5.91 (−10.74, −0.82)	−2.27	0.023
Lijiang City	3,856	9.71	Decrease	−4.02 (−6.00, −1.99)	−4.00	<0.001
Qujing City	18,613	9.52	Decrease	−2.18 (−3.92, −0.40)	−2.39	0.017
Diqing Tibetan Autonomous Prefecture	1,168	9.43	Stable	−11.89 (−15.18, −1.95)	−0.97	0.3319
Chuxiong Yi Autonomous Prefecture	7,768	8.82	Decrease	−7.18 (−10.55, −3.68)	−3.95	<0.001
Pu'er City	7,456	8.82	Decrease	−8.27 (−11.76, −4.64)	−4.53	<0.001
Zhaotong City	12,737	7.53	Decrease	−10.41 (−12.23, −8.55)	−10.89	<0.001
Lincang City	3,563	4.53	Decrease	−5.09 (−6.82, −3.33)	−5.78	<0.001

Abbreviation: *CI*s=confidence intervals.

Table S1 (available at https://weekly.chinacdc.cn/) presents the statistically significant H-H spatial clusters of TPF incidence in a total of 13 county-level cities/counties/municipal districts of 5 prefectures (cities) in Yunnan Province from 2005 to 2022 and the statistically significant L-L spatial clusters of TPF incidence in a total of 22 county-level cities/counties/municipal districts of 8 prefectures (cities) in Yunnan Province from 2005 to 2022.

Outbreaks

From 2005 to 2022, Yunnan Province reported 24 TPF outbreaks (12 typhoid fever and 12 paratyphoid fever), with a median duration of 21 days (Supplementary Table S2, available at https://weekly.chinacdc.cn/). These outbreaks involved 1,273 cases, an exposed population of 203,519, and an incidence rate of approximately 625.49 per 100,000. Occurring in 14 counties (districts) across 7 prefectures (cities) in Yunnan Province, the outbreaks primarily affected rural areas (17 outbreaks) and schools (6 outbreaks).

CONCLUSIONS

The overall TPF incidence in Yunnan Province, China, shows a significant decrease, potentially attributable to national disease prevention and control policies, public health service development, the inclusion of rural water and latrine improvements in disease prevention and control agencies' national code of practice (*8*), immunization, and improved sanitation and hygiene awareness (*9*). Despite annual declines in TPF incidence rates both nationally and in China, Yunnan Province remains the highest-ranking provincial-level administrative division (PLAD) for these diseases (*2*). The emergence of TPF as a significant public health issue in Yunnan Province highlights the critical need for effective epidemic control measures. Successfully managing the TPF epidemic in Yunnan Province is pivotal in diminishing the overall incidence of these diseases across China. Indeed, several possible reasons may explain the highest TPF incidence in Yunnan Province. First, Yunnan Province experiences peak TPF incidence during summer due to high temperatures and rainfall, creating ideal conditions for disease transmission (*9*–*10*). Second, abundant karst landforms in Yunnan Province increase the vulnerability of underground water sources to pathogenic bacterial contamination, amplifying the risk of TPF epidemics (*2*,*9*). Third, the epidemic's cause may also stem from differences in dietary and water hygiene practices among populations in Yunnan Province's multiethnic areas (*11*).

From 1989 to 2022, the top five average annual

incidences of TPF were observed in Xishuangbanna Dai Autonomous Prefecture, Dehong Dai-Jingpo Autonomous Prefecture, Yuxi City, Nujiang Lisu Autonomous Prefecture, and Honghe Hani and Yi Autonomous Prefecture. The four prefectures, excluding Yuxi City, are border prefectures with a high concentration of ethnic minorities. The elevated TPF incidence in these areas could be linked to prolonged case accumulation, heightened exposure rates, and changes in dietary and drinking practices among ethnic minorities (*11*). Additionally, the high TPF incidence between border county-level cities/counties/municipal districts in these prefectures (cities), such as Kunming City, Yuxi City, Honghe Hani and Yi Autonomous Prefecture, and Wenshan Zhuang and Miao Autonomous Prefecture, may be attributed to similar risk factors and provides a hypothesis for cross-regional transmission (*12*). The high incidence among farmers, students, and children is consistent with the findings of a national study (*12*) and may be linked to poor living conditions, increased outdoor exposure, and inadequate dietary and hygiene practices.

However, this study has limitations. First, data on TPF cases were acquired from the CISDCP infectious disease surveillance system via passive surveillance, potentially introducing reporting bias (*3*). Second, differences in testing, diagnostic, and reporting capabilities of hospitals at different levels in various regions lead to bias in identifying and reporting TPF. Third, the spatial autocorrelation analysis scale selection depends on the researcher's subjective judgment and does not consider the temporal characteristics of clustering; false positives are inevitable, so these results should be interpreted cautiously. Finally, this study did not include driving factors (e.g., pathogen resistance) and facilitating factors (e.g., meteorology) (*10*) that may influence TPF incidence; therefore, the causes of TPF incidence could not be analyzed. In conclusion, while the reported TPF incidence in Yunnan Province has decreased notably, it remains high, with noticeable spatial clustering in certain prefectures (cities).

Conflicts of interest: No conflicts of interest.

doi: 10.46234/ccdcw2024.216

[#] Corresponding authors: Jibo He, 5706343@qq.com; Weijun Yu, lncdcywj@163.com.

[1] Epidemic Surveillance/Public Health Emergency Response Center, Yunnan Provincial Center for Disease Control and Prevention, Kunming City, Yunnan Province, China; [2] Department of Intervention Research, Yunnan Institute for Drug Abuse, Kunming City, Yunnan Province, China; [3] Hunnan District Center for Disease Control and Prevention, Shenyang City, Liaoning Province, China; [4] Institute for Prevention and Control of Infection and Infectious Diseases, Liaoning Provincial Center for Disease Control and Prevention, Shenyang City, Liaoning Province, China.

[&] Joint first authors.

Submitted: April 22, 2024; Accepted: September 22, 2024

REFERENCES

1. GBD 2017 Typhoid and Paratyphoid Collaborators. The global burden of typhoid and paratyphoid fevers: a systematic analysis for the Global Burden of Disease Study 2017. Lancet Infect Dis 2019;19(4):369 – 81. https://doi.org/10.1016/S1473-3099(18)30685-6.
2. Gao XY, Tang QY, Liu FF, Song Y, Zhang ZJ, Chang ZR. Epidemiological characteristics of typhoid fever and paratyphoid fever in China, 2004-2020. Chin J Epidemiol 2023;44(5):743 – 50. https://doi.org/10.3760/cma.j.cn112338-20221116-00977.
3. Yu WJ, Guo LN, Shen XL, Wang ZJ, Cai J, Liu HH, et al. Epidemiological characteristics and spatiotemporal clustering of scarlet fever in Liaoning Province, China, 2010-2019. Acta Trop 2023;245:106968. https://doi.org/10.1016/j.actatropica.2023.106968.
4. Ministry of Health of the People's Republic of China. National public health emergency information reporting and management specification. Gaz Natl Health Comm People's Repub China 2006;(1):44-60. https://d.wanfangdata.com.cn/periodical/ChlQZXJpb2RpY2FsQ0hJTmV3UzIwMjQwNzA0Eg5RSzIwMDYwMzcwMzk0MRoIbnptbnc2Nmo%3D. (In Chinese).
5. Kim HJ, Fay MP, Feuer EJ, Midthune DN. Permutation tests for joinpoint regression with applications to cancer rates. Stat Med 2000;19(3):335 – 51. https://doi.org/10.1002/(SICI)1097-0258(20000215)19:3<335::AID-SIM336>3.0.CO;2-Z.
6. Yang SG, Wu J, Ding C, Cui YX, Zhou YQ, Li YP, et al. Epidemiological features of and changes in incidence of infectious diseases in China in the first decade after the SARS outbreak: an observational trend study. Lancet Infect Dis 2017;17(7):716 – 25. https://doi.org/10.1016/S1473-3099(17)30227-X.
7. Mahara G, Wang C, Huo D, Xu Q, Huang FF, Tao LX, et al. Spatiotemporal pattern analysis of scarlet fever incidence in Beijing, China, 2005-2014. Int J Environ Res Public Health 2016;13(1):131. https://doi.org/10.3390/ijerph13010131.
8. Jin T, Tao Y. The position and role of disease prevention and control institutions in safe drinking water and sanitary washroom work in rural areas. Chin Health Serv Manage, 2005;21(12):753 – 4. https://doi.org/10.3969/j.issn.1004-4663.2005.12.024.
9. Li RX, Liang YT, Yang N, Su YJ, Chen XL, Li H, et al. Epidemic characteristics of the changing trend of typhoid and paratyphoid in Chinese Mainland from 2004 to 2018. Chin J Dis Control Prev 2023;27(6):733 – 40. https://doi.org/10.16462/j.cnki.zhjbkz.2023.06.020.
10. Meng YP, Wang SK. Risk factors, early detection and effective surveillance of outbreaks or epidemics of typhoid and paratyphoid fevers: a review. Chin J Public Health 2022;38(3):371 – 5. https://doi.org/10.11847/zgggws1134365.
11. Chen YJ. Definitive diagnosis and risk factors for typhoid and paratyphoid in the endemic area of Yunnan province, China [dissertation]. Kunming: Kunming Medical University; 2014. https://kns.cnki.net/kcms2/article/abstract?v=K-Um1AVqjsLkktF6Rdlnisrs_EYG9saQIqpn-QFNoDpki1zxf8uKdYBP_oGUE8AIQDmXY3WwC0HFjE2t5z2jgvgT0t3pj8qp960-VUMCJ-YJpAd7ZTEZNw==&uniplatform=NZKPT&language=gb. (In Chinese).
12. Liu FF, Zhao SL, Chen Q, Chang ZR, Zhang J, Zheng YM, et al. Surveillance data on typhoid fever and paratyphoid fever in 2015, China. Chin J Epidemiol 2017;38(6):754 – 8. https://doi.org/10.3760/cma.j.issn.0254-6450.2017.06.013.

SUPPLEMENTARY MATERIAL

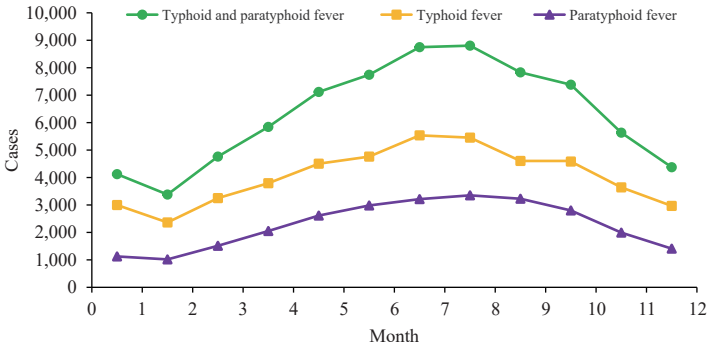

SUPPLEMENTARY FIGURE S1. Monthly reported cases of typhoid and paratyphoid fever in Yunnan Province, China, 2005–2022.

SUPPLEMENTARY TABLE S1. Statistically significant high-high and low-low spatial clusters of typhoid and paratyphoid fever in Yunnan Province, China, 2005–2022.

Year	High-High (H-H)	Low-Low (L-L)
2005–2010	Yuxi City (Jiangchuan District, Tonghai County, Huaning County and Eshan County), Kunming City (Chenggong District and Jinning District), Dehong Dai-Jingpo Autonomous Prefecture (Lianghe County and Ruili County-level City), and Xishuangbanna Dai Autonomous Prefecture (Jinghong County-level City).	Zhaotong City (Yanjin County, Yongshan County, Zhenxiong County, Yiliang County, Weixin County, and Shuifu County-level City), Lincang City (Linxiang District, Fengqing County, Yun County, Shuangjiang County, and Gengma County), Pu'er City (Ning'er County, Jinggu County, Zhenyuan County, and Jingdong County), Chuxiong Yi Autonomous Prefecture (Nanhua County, Chuxiong County-level City, and YaoAn County), Diqing Tibetan Autonomous Prefecture (Weixi County, Shangri-La County-level City, and Deqin County), Dali Bai Autonomous Prefecture (Nanjian County and Weishan County), Nujiang Lisu Autonomous Prefecture (Gongshan County and Lanping County), and Lijiang City (Gucheng District and Yulong Naxi Autonomous County).
2011–2016	Honghe Hani and Yi Autonomous Prefecture (Kaiyuan County-level City, Mengzi County-level City, Jianshui County, Mile County-level City, and Luxi County), Kunming City (Chenggong District, Yiliang County and Shilin County), Yuxi City (Huaning County), Wenshan Zhuang and Miao Autonomous Prefecture (Qiubei County), and Xishuangbanna Dai Autonomous Prefecture (Jinghong County-level City).	Zhaotong City (Zhaoyang District, Ludian County, Qiaojia County, Yanjin County, Daguan County, Yongshan County, Suijiang County, Zhenxiong County, Yiliang County, Weixin County, and Shuifu County-level City), Nujiang Lisu Autonomous Prefecture (Fugong County, Gongshan County and Lanping County), Chuxiong Yi Autonomous Prefecture (Chuxiong County-level City and Shuangbai County), Diqing Tibetan Autonomous Prefecture (Weixi County and Deqin County), Lincang City (Yun County), and Pu'er City (Jingdong County).
2017–2022	Honghe Hani and Yi Autonomous Prefecture (Kaiyuan County-level City, Mile County-level City, and Luxi County), Qujing City (Luliang County and Shizong County), Wenshan Zhuang and Miao Autonomous Prefecture (Yanshan County and Qiubei County), Lijiang City (Yongsheng County and Ninglang County), Kunming City (Shilin County), and Chuxiong Yi Autonomous Prefecture (Dayao County).	Zhaotong City (Yanjin County, Yongshan County, Suijiang County, Zhenxiong County, Yiliang County, Weixin County, and Shuifu County-level City), Lincang City (Yun County and Fengqing County), Nujiang Lisu Autonomous Prefecture (Fugong County and Gongshan County), Pu'er City (Mojiang County and Jingdong County), Yuxi City (Xinping County), Baoshan City (Shidian County), Chuxiong Yi Autonomous Prefecture (Chuxiong County-level City), Dali Bai Autonomous Prefecture (Nanjian County), and Diqing Tibetan Autonomous Prefecture (Deqin County).
2005–2022	Honghe Hani and Yi Autonomous Prefecture (Kaiyuan County-level City, Mengzi County-level City, Jianshui County, Mile County-level City, and Luxi County), Yuxi City (Jiangchuan District, Tonghai County, Huaning County, and Eshan County), Kunming City (Chenggong District and Jinning District), Dehong Dai-Jingpo Autonomous Prefecture (Ruili County-level City), and Xishuangbanna Dai Autonomous Prefecture (Jinghong County-level City).	Zhaotong City (Zhaoyang District, Yanjin County, Yongshan County, Zhenxiong County, Yiliang County, Weixin County, and Shuifu County-level City), Lincang City (Linxiang District, Fengqing County, Yun County, and Gengma County), Nujiang Lisu Autonomous Prefecture (Fugong County, Gongshan County and Lanping County), Pu'er City (Zhenyuan County and Jingdong County), Diqing Tibetan Autonomous Prefecture (Weixi County and Deqin County), Dali Bai Autonomous Prefecture (Nanjian County and Weishan County), Chuxiong Yi Autonomous Prefecture (Chuxiong County-level City), and Lijiang City (Yulong Naxi Autonomous County).

SUPPLEMENTARY TABLE S2. Typhoid and paratyphoid fever outbreaks in Yunnan Province, China, 2005–2022.

Year	Prefecture/City	County-level City/County/Municipal District	Outbreaks (*n*)	Cases (*n*)	Exposed population (*n*)	Incidence (%)
2005	Honghe Hani and Yi Autonomous Prefecture	Mile County-level City	2	83	2,206	3.76
2006	Qujing City	Luliang County	2	51	4,100	1.24
	Qujing City	Xuanwei County-level City	1	53	2,301	2.30
	Zhaotong City	Yongshan County	1	22	3,000	0.73
2007	Honghe Hani and Yi Autonomous Prefecture	Yuanyang County	1	19	548	3.47
	Yuxi City	Chengjiang County-level City	1	15	946	1.59
2008	Wenshan Zhuang and Miao Autonomous Prefecture	Maguan County	3	44	647	6.80
	Kunming City	Guandu District	1	92	3,026	3.04
	Zhaotong City	Yanjin County	1	18	454	3.96
2009	Honghe Hani and Yi Autonomous Prefecture	Gejiu County-level City	1	42	384	10.94
	Qujing City	Luliang County	1	34	386	8.81
	Qujing City	Shizong County	1	63	368	17.12
	Wenshan Zhuang and Miao Autonomous Prefecture	Maguan County	1	21	237	8.86
2010	Kunming City	Jinning District	1	13	2,500	0.52
2012	Wenshan Zhuang and Miao Autonomous Prefecture	Yanshan County	1	14	1,198	1.17
2014	Wenshan Zhuang and Miao Autonomous Prefecture	Yanshan County	2	559	178,592	0.31
2016	Baoshan City	Changning County	1	27	410	6.59
2017	Qujing City	Shizong County	1	49	2,076	2.36
	Wenshan Zhuang and Miao Autonomous Prefecture	Maguan County	1	14	140	10.00

Preplanned Studies

Monitoring the Status of Multi-Wave Omicron Variant Outbreaks — 71 Countries, 2021–2023

Chuanqing Xu[1,#]; Lianjiao Dai[1]; Songbai Guo[1]; Xiaoyu Zhao[2]; Xiaoling Liu[3]

Summary

What is already known about this topic?

Analyzing the characteristics of epidemic development after the emergence of the severe acute respiratory syndrome virus 2 Omicron variants with its subvariants and the impact of income level inequalities on the coronavirus disease 2019 (COVID-19) case-fatality ratio helps to better understand the spread of novel coronavirus infections.

What is added by this report?

The median time interval between the first and second waves of Omicron sub-variants was 70 days (interquartile spacing: 43.75–91), and between the second and third waves was 87.5 days (interquartile spacing: 49–119), which obeyed a lognormal distribution. The case-fatality ratio of the first wave was significantly higher than that of the second and third waves. During the initial epidemic period, there was no significant geographic differences in the case-fatality ratio of the first wave, while the case-fatality ratio in countries with high income levels was significantly lower than in countries with other income levels.

What are the implications for public health practice?

We still need to pay attention to the COVID-19 pandemic, as inequalities in income levels have an impact on the case-fatality ratio during the early stages of Omicron epidemics. In most countries, strains of the virus are likely to move from low to high population prevalence after 2–4 months.

The productive life of society has been greatly affected since the outbreak of coronavirus disease 2019 (COVID-19) in late 2019. In November 2021, genome surveillance teams in South Africa and Botswana detected the Omicron variant on November 26, 2021 (*1*). Compared to previous strains, the Omicron variant has a faster transmission rate and enhanced immune escape. Several scholars have shown that novel coronaviruses are characterized by multi-wave epidemics and changes in case-fatality ratios over time (*2–5*). Because of the multiple disparities between countries, differences in the number of confirmed cases and deaths in outbreaks across regions are often related to social inequalities (*6–7*). Ribeiro KB et al. studied social inequalities in COVID-19 mortality in São Paulo and showed that significant social inequalities exist in COVID-19 mortality, with higher case-fatality ratios among Black and mestizo populations compared to White populations and higher case-fatality ratios associated with lower socioeconomic indicators such as education and income (*8*). Perelman J et al. retrieved data from the Sixth National Health Survey of Portugal, conducted from September 2019 to December 2019, and examined and analyzed social inequalities in eight diseases associated with COVID-19 deaths in Portugal; they showed that populations with higher education had a lower risk of hypertension, diabetes, stroke, obesity, and cardiovascular disease (*9*). Since the naming of the Omicron strain, several waves of outbreaks have occurred in many countries, mainly caused by the Omicron strain and its variants. We collected epidemiological data on the Omicron variant of COVID-19 in 71 countries from November 14, 2021, to June 11, 2023, to analyze the characteristics of outbreak transmission following the emergence of the Omicron strain and assess the impact of income level inequalities on the COVID-19 case-fatality ratio.

This study compiled weekly data on new confirmed COVID-19 cases and deaths for 71 countries based on daily new COVID-19 cases published by the World Health Organization (https://covid19.who.int/data). The baseline was defined as the 50th percentile of the number of non-zero new weekly cases. The start of each outbreak wave was defined as the first of 3 consecutive weeks in which the number of new cases exceeded the baseline, and the end was defined as the first of 3 consecutive weeks in which the number of new cases fell below the baseline (*10*). Figure 1 shows the weekly trend of new cases between November 14, 2021, and June 11, 2023, using Poland, the United States, Singapore, and India as examples.

Based on World Bank classification criteria, the 71

countries were categorized by income level into four tiers: high-income, upper-middle-income, lower-middle-income, and low-income countries; and geographically into seven regions: South Asia, Europe and Central Asia, the Middle East and North Africa, East Asia and the Pacific, sub-Saharan Africa, North America, and Latin America and the Caribbean. The case-fatality ratio for each outbreak wave was calculated using the number of deaths divided by the number of confirmed cases during the same period. Descriptive statistics were analyzed for the time intervals between each outbreak wave. R 4.1.3 software (The R Foundation for Statistical Computing, Vienna, Austria) was used to conduct Fisher's exact test to determine whether country income level and geographic location were related to the number of outbreak waves. The Kruskal-Wallis one-way ANOVA was used to determine whether there was a significant difference in case-fatality ratios between different outbreak classifications and to assess the effect of income inequality on the outbreak case-fatality ratio.

Of the 71 countries included in the analysis, 5 experienced one wave of outbreaks, 22 experienced two waves, and 38 experienced three waves between November 14, 2021 and June 11, 2023. Six countries, including Brunei, Austria, and Uzbekistan, experienced four waves during this period.

Based on each epidemic wave's outbreak time and genomic surveillance data of COVID-19 from the Centers for Disease Control and Prevention, the predominant epidemiologic strains in the Omicron variant's first wave were BA.1.1, BA.2, and BA.2.12.1. The dominant viral strains in the second wave were BA.5, and the dominant strains in the third wave were

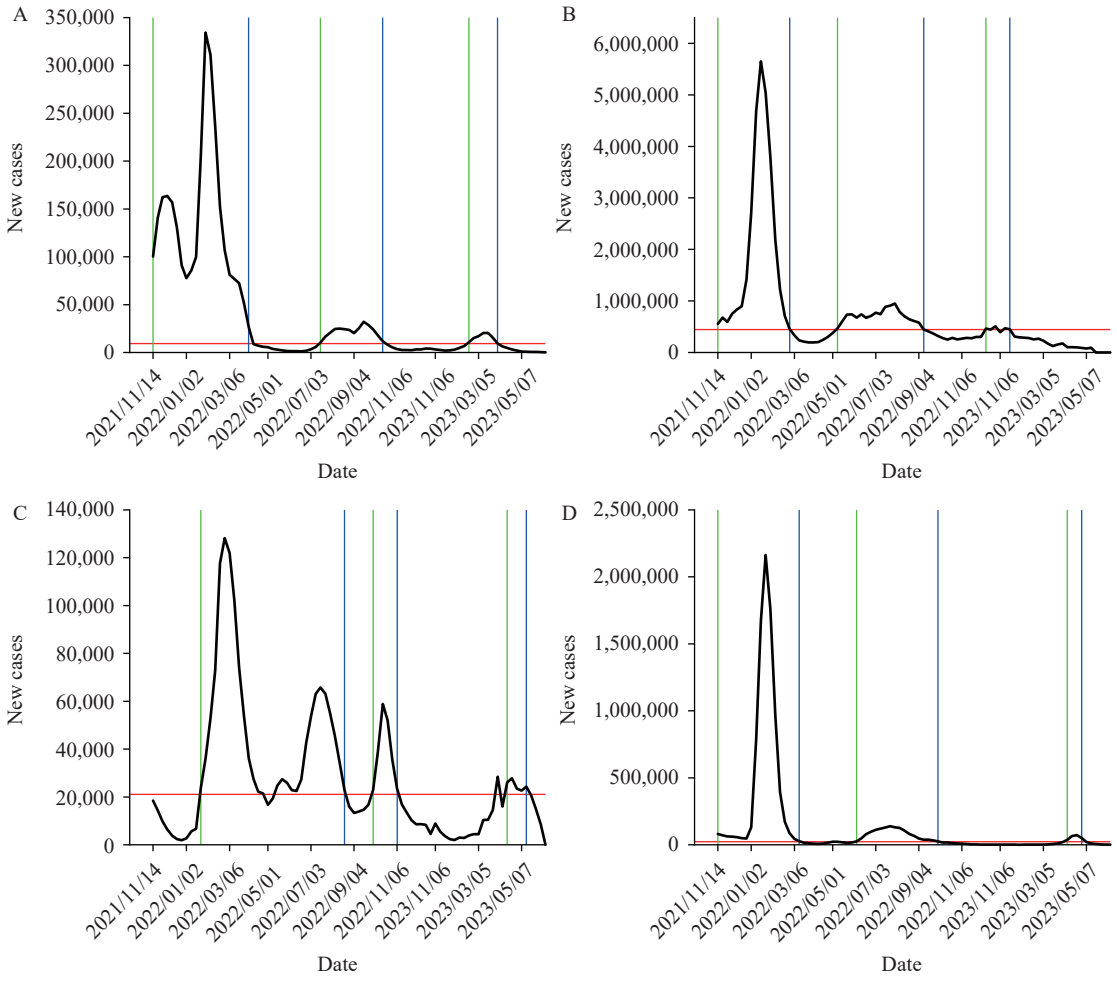

FIGURE 1. Time-series plot of new cases in (A) Poland, (B) the United States, (C) Singapore, and (D) India between November 14, 2021 and June 11, 2023.
Note: The black curve is the number of new confirmed cases per week, the red horizontal line is the baseline, the green vertical line is the start time of each wave of the epidemic, and the blue vertical line is the end time of each wave of the epidemic.

BQ.1.1 and XBB.1.5.

To obtain the time interval between low and high epidemics of the viral strains in the population, the interval between two waves of outbreaks was defined as the difference between the start time of each wave and the end time of the previous wave. The median interval between the first and second waves of Omicron subvariant outbreaks was 70 days (interquartile range: 43.75–91), and the median interval between the second and third waves was 87.5 days (interquartile range: 49–119); these intervals follow a lognormal distribution. These findings suggest that in most countries, the viral strain shows a trend of high prevalence approximately 2–4 months after the end of one wave. The distribution of the time interval between each outbreak wave is shown in Figure 2.

We studied the case-fatality ratio of Omicron variants over time and calculated the case-fatality ratio of outbreaks in 38 countries with three waves of outbreaks based on available data, as shown in Figure 3. We found that among the three epidemic waves, the highest case-fatality ratio occurred during the first wave of Omicron sub-variants in 24 countries: Greece, Chile, Singapore, Mexico, Guatemala, Peru, India, Ukraine, Kenya, Madagascar, Afghanistan, Ethiopia, Mali, Burundi, Italy, Switzerland, Panama, Poland, Qatar, Armenia, Ecuador, Morocco, Myanmar, and Plurinational State of Bolivia. The

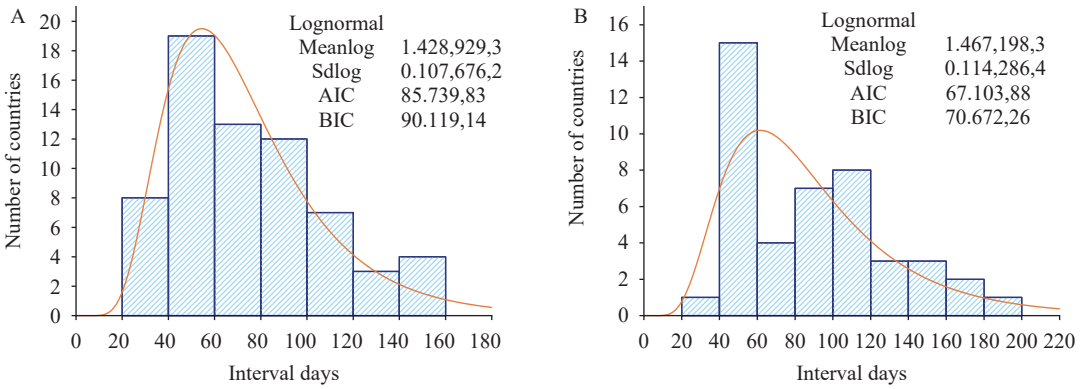

FIGURE 2. Distribution of outbreak intervals (A) between the first and second waves of Omicron sub-variants and (B) between the second and third waves.
Abbreviation: AIC=Akaike information criterion; BIC=Bayesian information criterion.

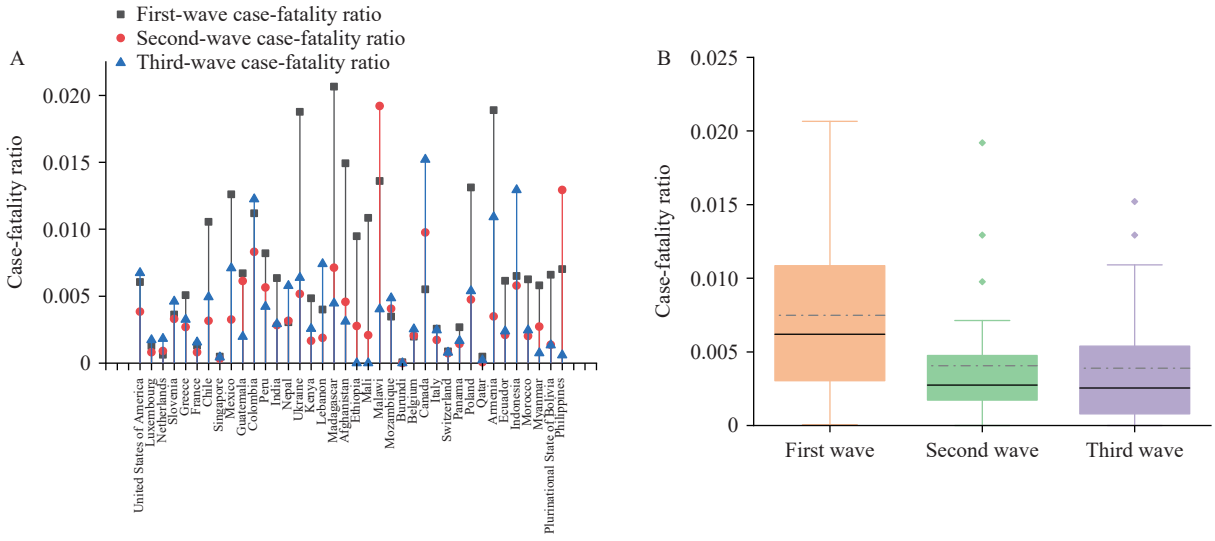

FIGURE 3. Case-fatality ratio analysis of three waves of outbreaks caused by Omicron variants in 38 countries. (A) Case-fatality ratio per country; (B) Case-fatality ratio per wave of the epidemic.
Note: In panel A, the black, red, and blue lines represent the first, second, and third waves of case-fatality ratios, respectively. In panel B, the solid line represents the median case-fatality rate for each wave of the epidemic, and the dashed line represents the mean case-fatality rate for each wave of the epidemic.

highest case-fatality ratio occurred in the second wave in two countries: Malawi and the Philippines. There were 12 countries with the highest case-fatality ratio in the third wave: the United States of America, Luxembourg, the Netherlands, Slovenia, France, Colombia, Nepal, Lebanon, Mozambique, Belgium, Canada, and Indonesia. The mean case-fatality ratios for these 38 countries in the three epidemic waves were 0.006899513, 0.003806385, and 0.003993398, respectively.

A Kruskal-Wallis one-way ANOVA was used to analyze differences in case-fatality ratios between epidemic waves. The resulting *P* value of 0.008572 was less than the 0.05 level of significance, indicating a significant difference in case-fatality ratios between the three epidemic waves. Dunn's method was used for pairwise comparisons. Results are shown in Table 1. The *P* value comparing the case-fatality ratio of the first wave to the second and third waves was less than 0.05. Box plots of the case-fatality ratios for the three waves show that the Omicron variant was associated with higher lethality in the early stages of emergence. As the pandemic progressed, the lethality of the second and third waves was much lower than that of the first wave of Omicron sub-variants.

Fisher's exact test was used to determine the correlation between a country's income level, geographic location, and the number of outbreak waves. The resulting *P* values were 0.7744 and 0.9219, respectively, indicating no relationship between a country's income level or geographic location and the number of outbreak waves. The case-fatality ratios from 71 countries experiencing the first wave of Omicron sub-variants were categorized by geographic location and analyzed using a Kruskal-Wallis one-way ANOVA. The *P* value of 0.2648 exceeded 0.05, indicating no significant difference in case-fatality ratios of the first Omicron sub-variant wave across regions. Figure 4A shows the case-fatality ratio levels of the first Omicron sub-variant wave according to a country's income class when the Omicron variant first circulated, addressing income inequality between countries. The mean case-fatality ratios of the first Omicron sub-variant wave for high-income, upper-middle-income, lower-middle-income, and low-income countries were 0.003053595, 0.009750986, 0.006429692, and 0.009294815, respectively.

TABLE 1. Results of Dunn's test for case-fatality ratio in three waves of the epidemic.

Comparison expression	Z	*P*
First wave *vs.* second wave	2.719	0.010
First wave *vs.* third wave	2.622	0.013
Second wave *vs.* third wave	−0.097	1.000

A Kruskal-Wallis one-way ANOVA was performed to assess the relationship between country income level and case-fatality ratio in the first wave of Omicron subvariants. This analysis was chosen based on sample size considerations. The *P* and Dunn's two-by-two comparison test results are shown in Table 2. These results indicate that, when the Omicron variant first became endemic, the case-fatality ratio was significantly lower in high-income countries compared to countries with other income levels. This difference is likely due to social inequalities and disparities in resource allocation.

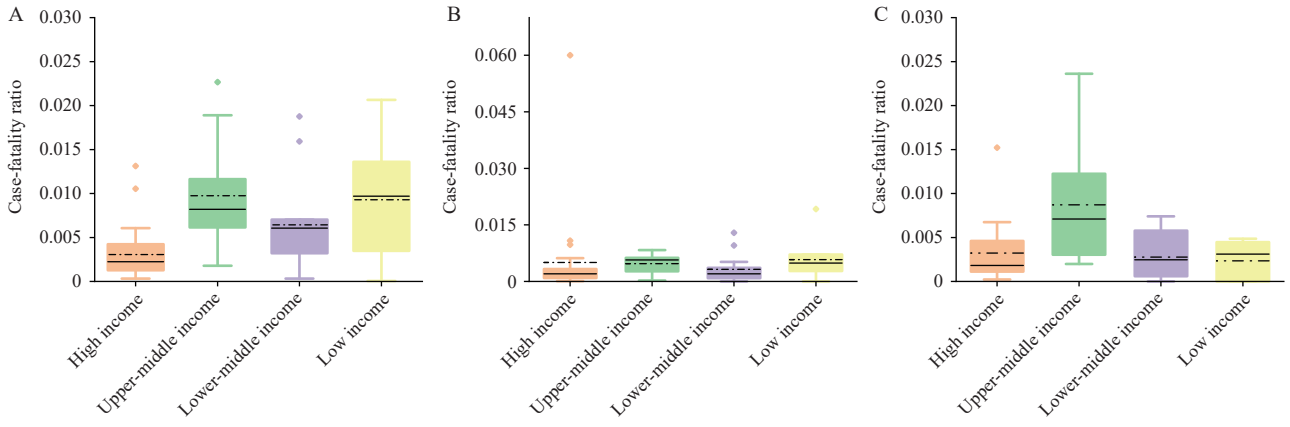

FIGURE 4. Levels of case-fatality ratio of Omicron sub-variants in countries with different income levels. (A) Levels of case-fatality ratio in the first wave of Omicron sub-variants in countries with different income levels. (B) Levels of case-fatality ratio in the second wave of Omicron sub-variants in countries with different income levels. (C) Levels of case-fatality ratio in the third wave of Omicron sub-variants in countries with different income levels.
Note: The solid line represents the median case-fatality rate for each wave of the epidemic, and the dashed line represents the mean case-fatality rate for each wave of the epidemic.

TABLE 2. Results of the Dunn's test for country income level and case-fatality ratio in the first wave of Omicron sub-variants.

Comparison expression	Z	P
High income *vs.* low income	−3.31	2.79×10^{-3}
High income *vs.* lower-middle income	−2.55	3.25×10^{-2}
Low income *vs.* lower-middle income	0.99	9.68×10^{-1}
High income *vs.* upper-middle income	−4.50	2.01×10^{-5}
Low income *vs.* upper-middle income	−0.02	1.00
Lower-middle income *vs.* upper-middle income	−1.60	3.32×10^{-1}

DISCUSSION

The constant mutation of COVID-19 strains and declining levels of immunity may cause coronaviruses to exhibit multiple epidemic waves. Our study found that neither the geographic location nor the income level of a country correlated with the number of epidemic waves. Although the Omicron variant of COVID-19 resulted in different case-fatality ratios for each epidemic wave, the second and third waves had significantly lower case-fatality ratios than the first wave.

Therefore, attention to the novel coronavirus epidemic remains paramount. Analysis of the data in this paper reveals that the interval between the end date of each wave and the start date of the next wave follows a lognormal distribution, with a median of 70 days (interquartile range: 43.75–91) and 87.5 days (interquartile range: 49–119), respectively. Consequently, most national viral strains will likely transition from low to high prevalence within 2–4 months. Discrepancies in income levels, resource allocation, and policy implementation across different countries contribute to significant variations in the Omicron case-fatality ratio. For instance, regarding vaccine distribution in Africa and the Middle East, countries with superior healthcare infrastructure have an advantage in vaccine access (*11*). Therefore, analyzing data from a wider range of countries and regions is crucial for a more accurate understanding of outbreak temporal characteristics. Increased immune escape by Omicron leads to multiple infection waves, and repeated infections increase the risk of death, hospitalization, and sequelae (*12*). Therefore, protective measures should be implemented to mitigate the risk of multiple novel coronavirus infections.

Conflicts of interest: No conflicts of interest.

Acknowledgements: Tengyi Xu (University of Waterloo) and all the individuals who generously shared their time and materials for this study.

Funding: Supported by the Guangdong Provincial Key Laboratory of Functional Substances in Medicinal Edible Resources and Healthcare Products (2021B1212040015), Natural Science Foundation of Shandong Province (ZR2023QA059), and the Pyramid Talent Training Project of BUCEA (JDYC20200327).

doi: 10.46234/ccdcw2024.218

[#] Corresponding author: Chuanqing Xu, xuchuanqing@bucea.edu.cn.

[1] School of Science, Beijing University of Civil Engineering and Architecture, Beijing, China; [2] School of Mathematics, Shandong University, Jinan City, Shandong Province, China; [3] Hanshan Normal University, Chaozhou City, Guangdong Province, China.

Submitted: March 19, 2024; Accepted: September 19, 2024

REFERENCES

1. Viana R, Moyo S, Amoako DG, Tegally H, Scheepers C, Althaus CL, et al. Rapid epidemic expansion of the SARS-CoV-2 Omicron variant in southern Africa. Nature 2022;603(7902):679 – 86. https://doi.org/10.1038/s41586-022-04411-y.
2. Su SY, Lee WC. Monitoring the peaks of multiwave COVID-19 outbreaks. J Microbiol Immunol Infect 2022;55(2):350 – 2. https://doi.org/10.1016/j.jmii.2021.07.005.
3. Fan GH, Yang ZC, Lin QY, Zhao S, Yang L, He DH. Decreased case fatality rate of COVID-19 in the second wave: a study in 53 countries or regions. Transbound Emerg Dis 2021;68(2):213 – 5. https://doi.org/10.1111/tbed.13819.
4. Vinceti M, Filippini T, Rothman KJ, Di Federico S, Orsini N. The association between first and second wave COVID-19 mortality in Italy. BMC Public Health 2021;21(1):2069. https://doi.org/10.1186/s12889-021-12126-4.
5. Liu J, Wei HZ, He DH. Differences in case-fatality-rate of emerging SARS-CoV-2 variants. Public Health Pract (Oxf) 2023;5:100350. https://doi.org/10.1016/j.puhip.2022.100350.
6. da Silva Nunes T, Soliman A, Taguchi K, Matsoso P, Driece RA, Tangcharoensathien V. Addressing inequity: the world needs an ambitious Pandemic Accord. Lancet 2023;402(10398):271 – 3. https://doi.org/10.1016/S0140-6736(23)01369-7.
7. Chilunga FP, Stoeldraijer L, Agyemang C, Stronks K, Harmsen C, Kunst AE. Inequalities in COVID-19 deaths by migration background during the first wave, interwave period and second wave of the COVID-19 pandemic: a closed cohort study of 17 million inhabitants of the Netherlands. J Epidemiol Community Health 2023;77(1):9-16. http://dx.doi.org/10.1136/jech-2022-219521.
8. Ribeiro KB, Ribeiro AF, de Sousa Mascena Veras MA, de Castro MC. Social inequalities and COVID-19 mortality in the city of São Paulo, Brazil. Int J Epidemiol 2021;50(3):732 – 42. https://doi.org/10.1093/ije/dyab022.
9. Perelman J. Syndemic pandemic in Portugal: social inequality in risk factors associated with COVID-19 Mortality. Acta Med Port 2022;35(6):443-9. https://doi.org/10.20344/amp.16031. (In Portuguese).
10. Yang W, Cowling BJ, Lau EH, Shaman J. Forecasting influenza epidemics in Hong Kong. PLoS Comput Biol 2015;11(7):e1004383. https://doi.org/10.1371/journal.pcbi.1004383.
11. Bizri AR, Al Akoury N, Mhlanga T, Morales GDC, Haridy H, Hussey GD, et al. The COVID-19 experience in Africa and the Middle East. Ann Med 2023;55(1):2222641. https://doi.org/10.1080/07853890.2023.2222641.
12. Bowe B, Xie Y, Al-Aly Z. Acute and postacute sequelae associated with SARS-CoV-2 reinfection. Nat Med 2022;28(11):2398 – 405. https://doi.org/10.1038/s41591-022-02051-3.

Methods and Applications

Impact of COVID-19 Interventions on Respiratory and Intestinal Infectious Disease Notifications — Jiangsu Province, China, 2020–2023

Ziying Chen[1]; Xin Liu[1]; Jinxing Guan[1]; Yingying Shi[2]; Wendong Liu[2]; Zhihang Peng[3,#]; Jianli Hu[1,2,4,#]

ABSTRACT

Introduction: Many measures implemented to control the coronavirus disease 2019 (COVID-19) pandemic have reshaped the epidemic patterns of other infectious diseases. This study estimated the impact of the COVID-19 pandemic on respiratory and intestinal infectious diseases and potential changes following reopening.

Methods: The optimal intervention and counterfactual models were selected from the seasonal autoregressive integrated moving average (SARIMA), neural network autoregression (NNAR), and hybrid models based on the minimum mean absolute percentage error (MAPE) in the test set. The relative change rate between the actual notification rate and that predicted by the optimal model was calculated for the entire COVID-19 epidemic prevention period and the "reopening" period.

Results: Compared with the predicted notification rate based on the counterfactual model, the total relative change rates for the 9 infectious diseases were –44.24%, respiratory infections (–55.41%), and intestinal infections (–26.59%) during 2020–2022. Compared with the predicted notification rate based on the intervention model, the total relative change rates were +247.98%, respiratory infections (+389.59%), and intestinal infections (+50.46%) in 2023. Among them, the relative increases in influenza (+499.98%) and hand-foot-mouth disease (HFMD) (+70.97%) were significant.

Conclusions: Measures taken in Jiangsu Province in response to COVID-19 effectively constrained the spread of respiratory and intestinal infectious diseases. Influenza and HFMD rebounded significantly after the lifting of COVID-19 intervention restrictions.

Since 2020, China has classified coronavirus disease 2019 (COVID-19) as a Category B infectious disease but managed it as a Category A disease, empowering local authorities to impose lockdowns and other stringent control measures (*1*). These COVID-19 control measures in China have persisted for nearly 3 years and may have far-reaching consequences for the healthcare system and other disease burdens. In January 2023, the Chinese government substantially adjusted its control policies, completely lifting COVID-19 interventions and resuming normal social and economic activities. The first COVID-19 case was confirmed in Jiangsu Province on January 22, 2020 (*2*). Several studies have shown that these measures are effective against COVID-19 and numerous other common infectious diseases, particularly respiratory and intestinal infections (*3*). Currently, the impacts of COVID-19 interventions on the spread of other respiratory and intestinal diseases in Jiangsu Province have been inconsistent.

Therefore, in this study, we established COVID-19 intervention models and counterfactual models of 9 respiratory and intestinal infectious diseases by adopting the seasonal autoregressive integrated moving average (SARIMA), neural network autoregression (NNAR), and hybrid models. We then compared the actual notification rate with the predicted rate and analyzed the impact of COVID-19 intervention measures in Jiangsu Province. This study aimed to provide a decision-making basis for the prevention and control of emerging infectious diseases.

METHODS

Data Source

Data on respiratory and intestinal infectious diseases between January 2004 and December 2023 in Jiangsu Province were obtained from the nationwide Notifiable Infectious Diseases Reporting Information System (NIDRIS). Based on the criterion of an annual average number of reported cases exceeding 250 from 2020 to

2022, a total of nine notifiable infectious diseases were identified for analysis: tuberculosis, influenza, mumps, scarlet fever, hepatitis A, dysentery, infectious diarrhoeal diseases other than cholera, dysentery, and typhoid/paratyphoid (OID), hand-foot-mouth disease (HFMD), and hepatitis E.

This study used the overall government response index from the Oxford COVID-19 Government Response Tracker (OxCGRT) to quantify COVID-19 interventions (*4*). This index tracks the strength and variation of all relevant indicators of government response from 2020 to 2022 on a scale of 0 to 100.

Establishment of the SARIMA Model

SARIMA, a variant of the ARIMA model, is expressed as SARIMA$(p,d,q)(P,D,Q)s$ (*5*). The parameters p, d, and q represent the orders of autoregression, the degree of trend difference, and the moving average for the nonseasonal component, respectively. P signifies the order of seasonal autoregression; D, the degree of seasonal difference; Q, the order of the seasonal moving average; and s, the seasonal period.

Establishment of the NNAR Model

NNAR models can be conceptualized as a complex network of neurons or nodes, exhibiting intricate nonlinear interactions and functional forms. The model can be described with the notation NNAR$(p,P,k)m$ for seasonal data, where p represents the number of nonseasonal lagged inputs for the linear autoregressive (AR) model process, P denotes the seasonal lag for the AR model process, k signifies the number of nodes in the hidden layer, and m is the length of the seasonal period (*5*).

Establishment of The SARIMA-NNAR Hybrid Model

A hybrid model was constructed by combining the SARIMA and NNAR models with equal weights.

Model Evaluations

We used a quantitative metric to evaluate and compare the performance of the models: MAPE. The formula used to calculate the metric is shown below (*6*):

$$MAPE = \frac{1}{n}\sum_{t=1}^{n}\frac{|y_t - \hat{y}_t|}{y_t}$$

where y_t and $\hat{y}_t$ denote the original and predicted values at time t, respectively, and n is the number of predictions. A model with small mean absolute percentage error (MAPE) values is preferred.

Constructing the Counterfactual Models

The SARMA, NNAR, and hybrid models were used to construct counterfactual models. Monthly case counts for each infectious disease from 2004 to 2017 served as the training set, while data from 2018 to 2019 served as the test set. The baseline models with the lowest MAPE values on the test set were selected and trained using data from 2004 to 2019 to predict case counts from 2020 to 2023.

Constructing the COVID-19 Intervention Models

Three models were constructed using monthly case counts for each infectious disease and overall government response indices. Data from 2004 to 2021 were used for model training and construction, while data from 2022 served as the test set to assess model performance. The best baseline models were selected based on the minimum MAPE value obtained from the test set. Subsequently, these models were trained using data from 2004 to 2022 to predict the number of cases in 2023 (Supplementary Figure S1, available at https://weekly.chinacdc.cn/).

RESULTS

Selection of The Optimal Model

The counterfactual models were neural network for tuberculosis, influenza, and OID; SARMA for mumps, scarlet fever, and HFMD; and hybrid for hepatitis A, dysentery, and hepatitis E. The intervention models were hybrid for tuberculosis, mumps, scarlet fever, dysentery, OID, HFMD, and hepatitis E; neural network for influenza; and SARIMA for hepatitis A. (Supplementary Table S1, available at https://weekly.chinacdc.cn/)

Predicted Yearly Notification Rates for 2020–2023 Based on Counterfactual Models

The actual yearly notification rates for 9 infectious diseases from 2020 to 2022 were lower than the rates predicted by the counterfactual models. The total relative change rates for the 9 infectious diseases, respiratory infections, and intestinal infections were

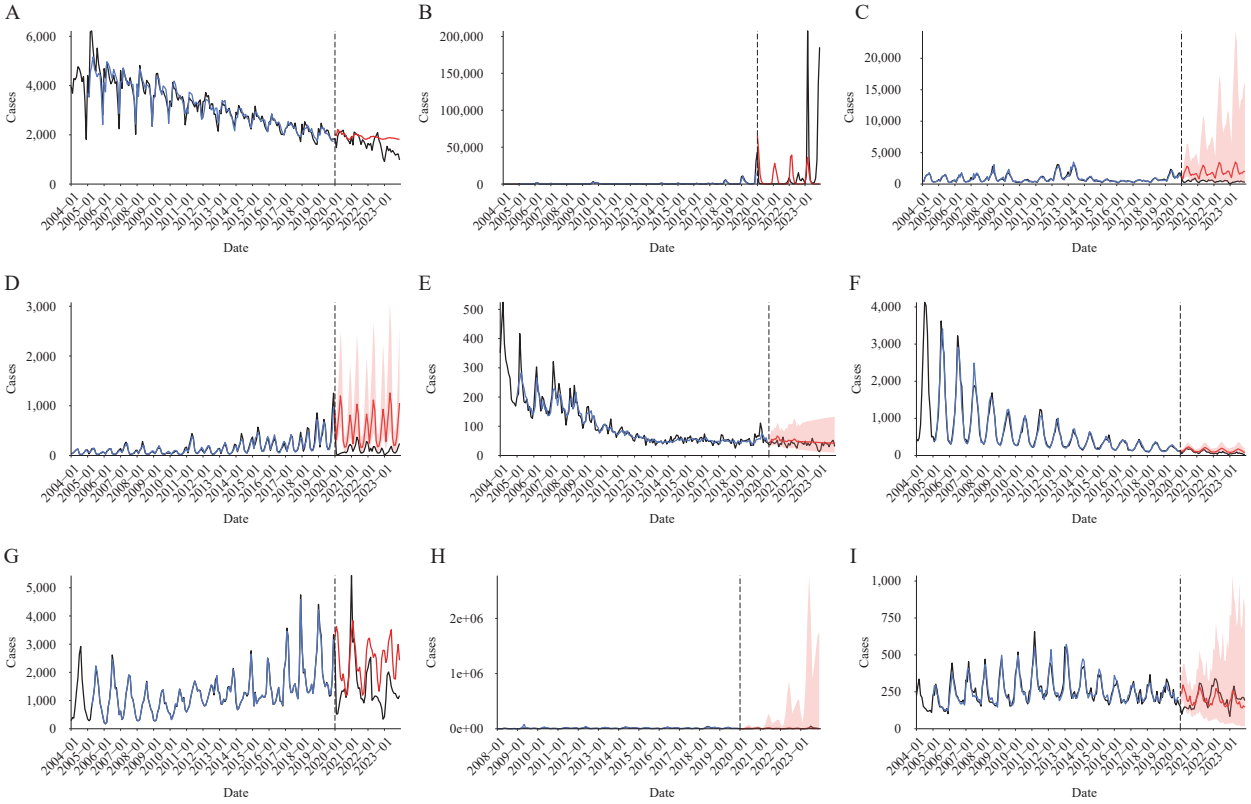

FIGURE 1. The observed notification rate versus the predicted notification rate based on 2020–2023 according to the counterfactual model. (A) Tuberculosis; (B) Influenza; (C) Mumps; (D) Scarlet fever; (E) Hepatitis A; (F) Dysentery; (G) OID; (H) HFMD; (I) Hepatitis E.
Note: The blue line represents the fitted values, the black line represents the actual values, and the red line along with the pink area represents the predicted values and the 95% confidence interval, respectively.
Abbreviation: OID=infectious diarrhoeal diseases other than cholera, dysentery, and typhoid/paratyphoid; HFMD=hand-foot-mouth disease.

–44.24%, –55.41%, and –26.59%, respectively. The three diseases with the highest relative change rates were scarlet fever (–75.90%), mumps (–73.35%), and influenza (–61.00%). (Figure 1 and Table 1)

The total notification rates for 9 infectious diseases in 2023 predicted by the COVID-19 intervention model and the counterfactual model were similar (P=0.796).

Predicted Yearly Notification Rates for 2023 Based on COVID-19 Intervention Models

The actual yearly notification rate of 9 infectious diseases in 2023 was higher than the rate predicted by the COVID-19 intervention model, which incorporates the overall government response index to reflect changes in non-pharmaceutical interventions (NPIs). The total relative change rate for the 9 infectious diseases was +247.98%, with respiratory infections (+389.59%) and intestinal infections (+50.46%) showing increases. Three infectious diseases — influenza (+499.98%), HFMD (+70.97%), and hepatitis A (+7.04%) — showed a relative increase, while the remaining 6 infectious diseases showed a relative reduction (Figure 2 and Table 1).

DISCUSSION

COVID-19 intervention measures effectively curbed the spread of respiratory and enteric infectious diseases in Jiangsu. We observed that the incidence of 9 infectious diseases declined compared to model predictions during 2020–2022, and the reduction in respiratory infectious diseases was greater than that in intestinal infectious diseases.

The lifting of NPIs did not result in a rebound of all infectious diseases; only influenza and HFMD infections were significantly higher than predicted by the intervention model. Similar observations have been reported in other countries. In late 2022, a surge in influenza and respiratory syncytial virus infections in

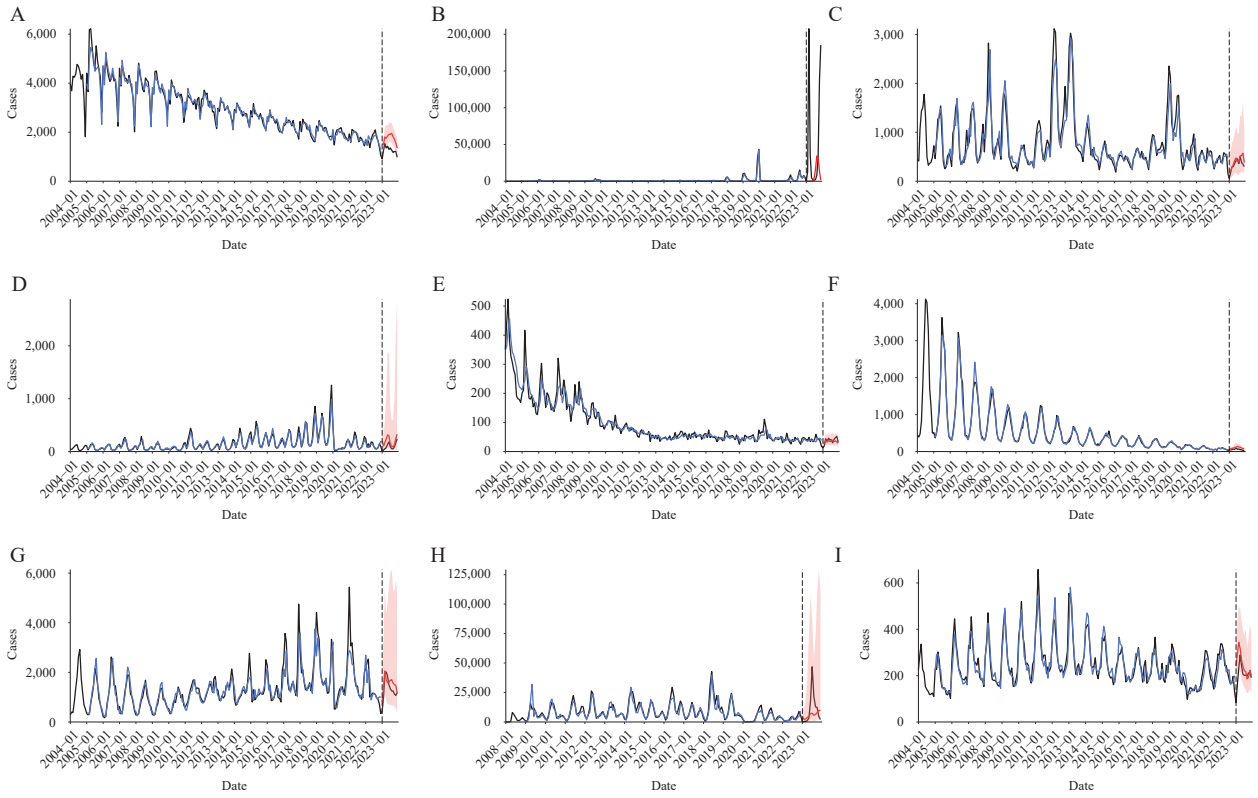

FIGURE 2. The observed notification rate versus the predicted notification rate based on 2023 according to the intervention model. (A) Tuberculosis; (B) Influenza; (C) Mumps; (D) Scarlet fever; (E) Hepatitis A; (F) Dysentery; (G) OID;(H) HFMD; (I) Hepatitis E.
Note: The blue line represents the fitted values, the black line represents the actual values, and the red line along with the pink area represents the predicted values and the 95% confidence interval, respectively.
Abbreviation: OID=infectious diarrhoeal diseases other than cholera, dysentery, and typhoid/paratyphoid; HFMD=hand-foot-mouth disease.

the U.S. led to numerous reports (*7*). This wave of respiratory infections among children coincided with the easing of COVID-19 restrictions. Similarly, the incidence of HFMD rebounded in Japan as NPIs were relaxed (*8*). Based on current data, the observed rebounds or outbreaks following the easing of NPIs initially appeared in children and were all attributed to non-vaccine preventable diseases (non-VPDs) (*9*). However, given the potential decline in community immunity due to disruptions in vaccination programs during the COVID-19 pandemic (*10*), similar rebound trends observed for non-VPDs might also be anticipated for VPDs.

Some medical professionals and media outlets use the term "immune debt" to explain the surge in influenza and HFMD cases in 2023 (*11*), referring to the lack of pathogen exposure that leaves immune systems less prepared to fight these diseases. However, opponents argue that the immune system does not operate on a "use it or lose it" mechanism; even without exposure to pathogens, the human immune system maintains normal natural immunity (*12*). Indeed, several scholars have proposed new explanations for this phenomenon: the severe acute respiratorysyndrome virus 2 (SARS-CoV-2) virus damages the immune system through T-cell responses, weakening resistance to common infectious diseases (*13*). Immune dysfunction can persist for up to 8 months, even in patients with mild to moderate SARS-CoV-2 infection (*14*). However, further evidence is needed to confirm this viewpoint.

Most related studies have focused on assessing the impact of COVID-19 outbreaks and control measures on other infectious diseases during the early stages of lockdown or specific periods. This study encompasses the entire COVID-19 period and considers the dynamic changes in NIPs. We selected optimal models to improve prediction accuracy, retrospectively analyzed and compared case reports, and addressed inquiries regarding the magnitude of changes in respiratory and intestinal infectious diseases after the cancellation of the zero-clearing policy in a timely

TABLE 1. The predicted yearly notification rate based on the counterfactual model and the intervention model from 2020 to 2023.

Disease category	Diseases	Counterfactual model						Intervention model		
		2020–2022			2023			2023		
		cases (*n*)	Average annual incidence (1/100,000)	relative change rate of incidence (%)	cases (*n*)	Annual incidence (1/100,000)	relative change rate of incidence (%)	cases (*n*)	Annual incidence (1/100,000)	relative change rate of incidence (%)
Respiratory	Tuberculosis	69,823	27.87	−7.79	22,229	26.10	−32.46	20,661	24.26	−27.34
	Influenza	304,717	121.64	−61.00	83,959	98.60	649.72	104,913	123.20	499.98
	Mumps	67,543	26.96	−73.35	25,371	29.79	−84.35	4,738	5.56	−16.19
	Scarlet fever	19,979	7.98	−75.90	7,577	8.90	−84.51	2,373	2.79	−50.53
	Total	462,062	184.46	−55.41	139,136	163.39	366.89	132,685	155.82	389.59
Intestinal	Hepatitis A	1,796	0.72	−18.44	517	0.61	−14.89	411	0.48	7.04
	Dysentery	5,262	2.10	−34.49	1,452	1.71	−55.03	1,184	1.39	−44.85
	OID	85,067	33.96	−32.22	31,469	36.96	−49.39	18,250	21.43	−12.73
	HFMD	192,943	77.02	−24.95	58,830	69.09	110.24	72,341	84.95	70.97
	Hepatitis E	7,348	2.93	−0.75	2,225	2.61	9.48	2,947	3.46	−17.34
	Total	292,416	116.73	−26.59	94,493	110.97	51.48	95,133	111.72	50.46
Total		754,478	301.19	−44.24	233,629	274.36	239.32	227,818	267.54	247.98

Note: relative change rate of incidence=(actual incidence−predicted incidence)/predicited incidence.

manner.

Our study has certain limitations. First, the lower number of reported cases of certain infectious diseases than predicted during the three-year COVID-19 intervention may reflect underreporting due to reluctance to seek medical care, potentially biasing reporting data and underestimating the actual incidence. Second, most OxCGRT data indicators are based on the strictest government policies implemented in a single country, which may limit the generalizability of our findings to other countries or regions with less stringent measures.

Funding: This study was supported by grants from the Jiangsu Provincial Medical Key Discipline (No. ZDXK202250), the Scientific Research Project of Jiangsu Provincial Health Commission (No. DX202302), National Natural Science Foun dation of China (No. 82320108018) and National Key R&D Program of China (Nos. 2023YFC2306004, 2022YFC2304000).

doi: 10.46234/ccdcw2024.219

[#] Corresponding authors: Jianli Hu, jshjl@jscdc.cn; Zhihang Peng, zhihangpeng@njmu.edu.cn.

[1] School of Public Health, Nanjing Medical University, Nanjing City, Jiangsu Province, China; [2] Department of Acute Infectious Diseases Control and Prevention, Jiangsu Provincial Center for Disease Control and Prevention, Nanjing City, Jiangsu Province, China; [3] National Key Laboratory of Intelligent Tracking and Forecasting for Infectious Diseases, Chinese Center for Disease Control and Prevention, Beijing, China; [4] Jiangsu Province Engineering Research Center of Health Emergency, Nanjing City, Jiangsu Province, China.

Submitted: June 21, 2024; Accepted: September 19, 2024

REFERENCES

1. Iezadi S, Gholipour K, Azami-Aghdash S, Ghiasi A, Rezapour A, Pourasghari H, et al. Effectiveness of non-pharmaceutical public health interventions against COVID-19: a systematic review and meta-analysis. PLoS One 2021;16(11):e0260371. https://doi.org/10.1371/journal.pone.0260371.
2. Cheng XQ, Hu JL, Luo L, Zhao ZY, Zhang N, Hannah MN, et al. Impact of interventions on the incidence of natural focal diseases during the outbreak of COVID-19 in Jiangsu Province, China. Parasit Vectors 2021;14(1):483. https://doi.org/10.1186/s13071-021-04986-x.
3. Xiao JP, Dai JY, Hu JX, Liu T, Gong DX, Li X, et al. Co-benefits of nonpharmaceutical intervention against COVID-19 on infectious diseases in China: a large population-based observational study. Lancet Reg Health West Pac 2021;17:100282. https://doi.org/10.1016/j.lanwpc.2021.100282.
4. Cross M, Ng SK, Scuffham P. Trading health for wealth: the effect of COVID-19 response stringency. Int J Environ Res Public Health 2020;17(23):8725. https://doi.org/10.3390/ijerph17238725.
5. Perone G. Comparison of ARIMA, ETS, NNAR, TBATS and hybrid models to forecast the second wave of COVID-19 hospitalizations in Italy. Eur J Health Econ 2022;23(6):917 – 40. https://doi.org/10.1007/s10198-021-01347-4.
6. Zhang YY, Tang S, Yu G. An interpretable hybrid predictive model of

COVID-19 cases using autoregressive model and LSTM. Sci Rep 2023;13(1):6708. https://doi.org/10.1038/s41598-023-33685-z.
7. Abbasi J. "This is our COVID"—what physicians need to know about the pediatric RSV surge. JAMA 2022;328(21):2096 – 8. https://doi.org/10.1001/jama.2022.21638.
8. Ghaznavi C, Tanoue Y, Kawashima T, Eguchi A, Yoneoka D, Sakamoto H, et al. Recent changes in the reporting of STIs in Japan during the COVID-19 pandemic. Sex Transm Infect 2023;99(2):124 – 7. https://doi.org/10.1136/sextrans-2021-055378.
9. Oh KB, Doherty TM, Vetter V, Bonanni P. Lifting non-pharmaceutical interventions following the COVID-19 pandemic - the quiet before the storm? Expert Rev Vaccines 2022;21(11):1541-53. http://dx.doi.org/10.1080/14760584.2022.2117693.
10. Feldman AG, O'Leary ST, Danziger-Isakov L. The risk of resurgence in vaccine-preventable infections due to coronavirus disease 2019-related gaps in immunization. Clin Infect Dis 2021;73(10):1920 – 3. https://doi.org/10.1093/cid/ciab127.
11. Hatter L, Eathorne A, Hills T, Bruce P, Beasley R. Respiratory syncytial virus: paying the immunity debt with interest. Lancet Child Adolesc Health 2021;5(12):e44 – 5. https://doi.org/10.1016/s2352-4642(21)00333-3.
12. Pan QC, Chen XH, Yu YS, Zang GQ, Tang ZH. The outbreak of seasonal influenza after the COVID-19 pandemic in China: unraveling the "Immunity debt". Infect Dis Now 2024;54(1):104834. https://doi.org/10.1016/j.idnow.2023.104834.
13. Govender M, Hopkins FR, Göransson R, Svanberg C, Shankar EM, Hjorth M, et al. T cell perturbations persist for at least 6 months following hospitalization for COVID-19. Front Immunol 2022;13:931039. https://doi.org/10.3389/fimmu.2022.931039.
14. Phetsouphanh C, Darley DR, Wilson DB, Howe A, Munier CML, Patel SK, et al. Immunological dysfunction persists for 8 months following initial mild-to-moderate SARS-CoV-2 infection. Nat Immunol 2022;23(2):210 – 6. https://doi.org/10.1038/s41590-021-01113-x.

SUPPLEMENTARY MATERIAL

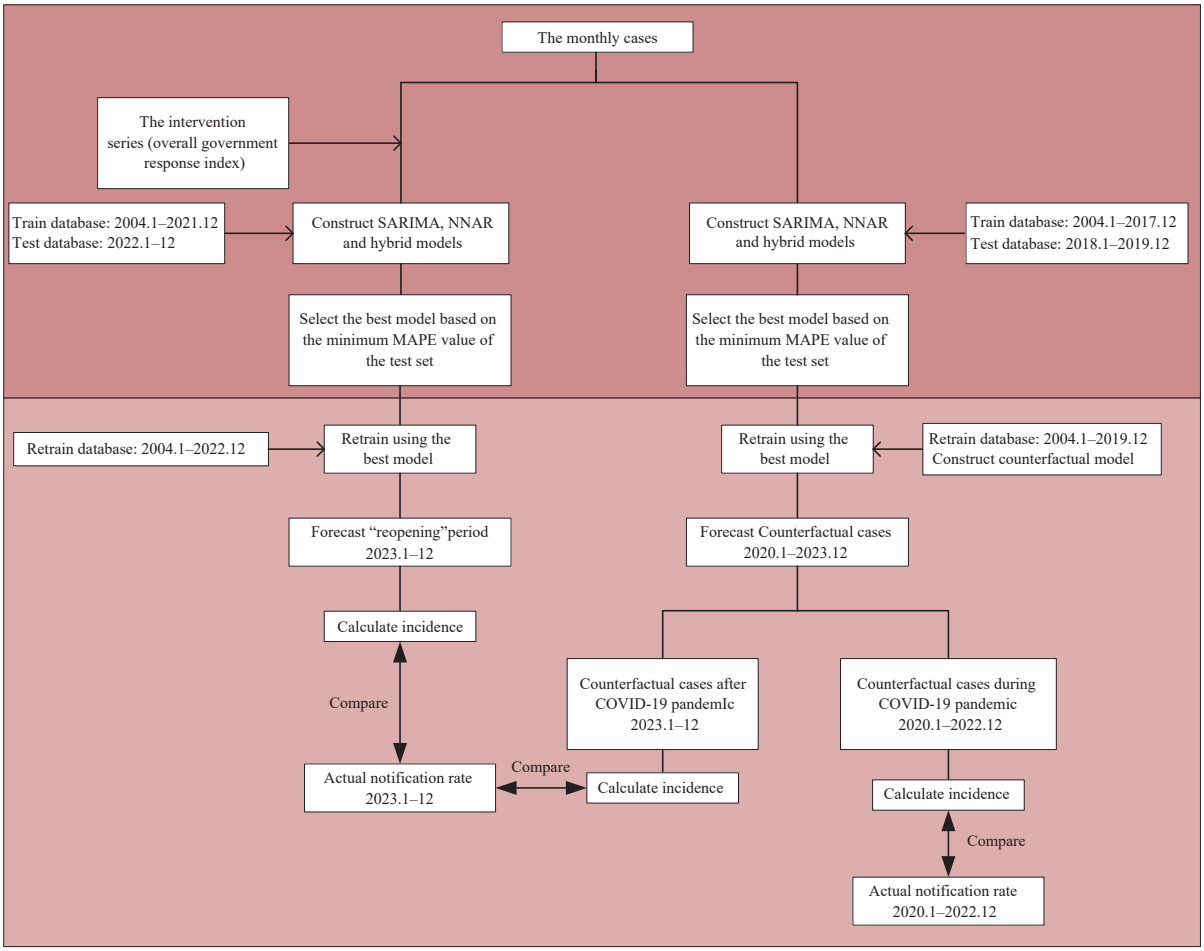

SUPPLEMENTARY FIGURE S1. Research design and model training diagram.
Abbreviation: SARIMA=seasonal autoregressive integrated moving average; NNAR=neural network autoregression; MAPE=mean absolute percentage error; COVID-19=coronavirus disease 2019.

SUPPLEMENTARY TABLE S1. Selection of optimal model.

Disease category	Diseases	Counterfactual model (The first step)		Intervention model (The second step)	
		Final model	Model parameter	Final model	Model parameter
Respiratory	Tuberculosis	Neural Network	NNAR(3,1,2)[12]	Hybrid	−
	Influenza	Neural Network	NNAR(13,1,7)[12]	Neural Network	NNAR(13,1,8)[12]
	Mumps	SARIMA	SARIMA(3,0,1)(2,1,0)[12]	Hybrid	−
	Scarlet fever	SARIMA	SARIMA(2,0,0)(0,1,1)[12]	Hybrid	−
Intestinal	Hepatitis A	Hybrid	−	SARIMA	SARIMA(0,1,3)(0,0,2)[12]
	Dysentery	Hybrid	−	Hybrid	−
	OID	Neural Network	NNAR(15,1,8)[12]	Hybrid	−
	HFMD	SARIMA	SARIMA(3,1,0)(0,1,1)[12]	Hybrid	−
	Hepatitis E	Hybrid	−	Hybrid	−

Note: "−" means SARIMA-NNAR (SARIMA with weight 0.5, NNAR with weight 0.5).
Abbreviation: SARIMA=seasonal autoregressive integrated moving average; NNAR=neural network autoregression; OID=infectious diarrhoeal diseases other than cholera, dysentery, and typhoid/paratyphoid; HFMD=hand-foot-mouth disease

Review

Drawing on the Development Experiences of Infectious Disease Surveillance Systems Around the World

Huimin Sun[1]; Weihua Hu[1]; Yongyue Wei[1]; Yuantao Hao[1,2,3,#]

ABSTRACT

High-quality infectious disease surveillance systems are foundational to infectious disease prevention and control. Current major infectious disease surveillance systems globally can be categorized as either indicator-based, which are more specific, or event-based, which are more timely. Modern surveillance systems commonly utilize multi-source data, strengthened information sharing, advanced technology, and improved early warning accuracy and sensitivity. International experience may provide valuable insights for China. China's existing infectious disease surveillance systems require urgent enhancements to monitor emerging infectious diseases and improve the integration and learning capabilities of early warning models. Methods such as establishing multi-stage surveillance systems, promoting cross-sectoral and cross-provincial data sharing, applying advanced technologies like artificial intelligence, and cultivating professional talent should be adopted to enhance the development of intelligent and multipoint-triggered infectious disease surveillance systems in China.

Throughout history, infectious diseases have caused enormous loss of life and social distress, and despite modern scientific and technological advances, they remain an ongoing threat. The emergence and re-emergence of infectious diseases serve as reminders of the need for constant vigilance. High-quality surveillance systems are crucial for the effective prevention and control of infectious diseases. By collecting and analyzing epidemic data, these systems detect infectious disease trends and provide early warnings of potential outbreaks, enabling authorities to take swift action and reduce the risk of disease transmission.

China implemented the National Notifiable Infectious Diseases Reporting Information System (NIDRIS) in 2004 to enable nationwide direct reporting of infectious diseases. In 2008, the China Infectious Diseases Automated-alert and Response System (CIDARS) launched, creating an automatic warning model based on NIDRIS data (*1*). These systems have helped address China's infectious disease surveillance and early warning challenges. However, over time, NIDRIS and CIDARS have encountered problems such as delayed warning checkpoints, limited information sources, and technologies in need of improvement (*2*). The inauguration of the National Bureau of Disease Control and Prevention in 2021 signified the start of reform for China's disease prevention and control system. Infectious disease surveillance, a pivotal responsibility of the CDC, is in urgent need of improvement. As President Xi Jinping emphasized, enhancing monitoring and early warning capabilities should be a top priority for a sound public health system. China requires intelligent and multi-point-triggered surveillance systems, which generally refer to advanced systems that leverage technologies such as big data, cloud computing, the Internet of Things, and artificial intelligence (AI) to automatically collect data, synthesize results, and issue early warnings from multiple critical nodes in the infectious disease lifecycle. Such systems also incorporate public opinion data from media and social networks, along with other sociologically relevant information about disease emergence, to improve the sensitivity, accuracy, and timeliness of early warnings, thereby reducing human error and oversight (*2*).

China can benefit from international experience in developing surveillance systems. This article reviews global experience with infectious disease surveillance systems to understand potential improvements for China's national surveillance system, aiming to provide insights for constructing intelligent, multipoint-triggered infectious disease surveillance systems in China.

OVERVIEW OF SURVEILLANCE SYSTEMS GLOBALLY

Infectious disease surveillance can be defined as continuously and systematically collecting information on infectious diseases and related factors and dynamically analyzing the temporal, spatial, and population distribution of infectious diseases to understand the current status and trends of infectious diseases and provide guidance for preventive and control measures (*3*). The main components of an infectious disease surveillance system include data collection, data management, data analysis, investigation, and reporting (*4*). Early warning identifies abnormal signals from surveillance data and then performs alert management, which involves managing and sorting these signals to ensure effective responses. Together, surveillance, early warning, alert management, and response form a comprehensive process that is critical to the timely detection and opportune management of infectious disease threats (*5*).

We searched PubMed, Web of Science, and China National Knowledge Infrastructure using the following search terms: (infectious disease OR communicable disease) AND (surveillance OR monitoring OR early warning) AND system. From the retrieved articles, we extracted specific information about each surveillance system, including system name, website, system type, country or region, year started, area of service, data sources, data access, functions, and features. We selected and summarized infectious disease surveillance systems from leading countries or regions, including the United States and Canada for North America, the European Union for Europe, China and Japan for Asia, and Australia for Oceania. According to the European CDC's methodological framework for epidemiological intelligence, infectious disease surveillance systems can be classified as indicator-based and event-based (*6*). Indicator-based systems collect structured data from routine surveillance like case numbers, morbidity, mortality, laboratory test results, and consumption of specific drugs. Event-based systems collect unstructured data from any formal or informal source and are mainly used in web-based surveillance systems such as the Program for Monitoring Emerging Diseases (ProMED) Mail, the Global Public Health Intelligence Network (GPHIN), and HealthMap (*7*–*8*).

Indicator-Based Surveillance Systems

Indicator-based surveillance systems are technologically mature and rely on passive reporting by healthcare organizations (Table 1). For instance, the United States' National Notifiable Diseases Surveillance System (NNDSS) (*9*), China's NIDRIS and CIDARS, and the European Surveillance System (TESSy) (*10*) are used to monitor cases of notifiable infectious diseases. The United States' Electronic Laboratory Reporting (ELR) systems and Japan's Infectious Agents Surveillance Report (IASR) monitor laboratory testing information (*11*). Before microbiological confirmation, syndromic surveillance collects and analyzes routine health-related data on symptoms and clinical signs, often from emergency departments and other healthcare settings (*12*–*13*). In the United States, the National Syndromic Surveillance Program (NSSP) has been instrumental in detecting and monitoring health threats by aggregating data from over 6,500 healthcare facilities across the country (*14*). In England, national real-time syndromic surveillance systems have been developed using data from telemedicine triage systems, general practice, and emergency departments to support early detection of seasonal influenza and situational awareness during public events (*15*).

In recent years, wastewater surveillance has emerged as a critical component of indicator-based surveillance systems. Klapsa and colleagues reported the detection of poliovirus isolates related to the serotype 2 Sabin vaccine strain in London sewage samples, demonstrating the potential of wastewater surveillance in identifying community transmission and genetic evolution of pathogens (*16*). Similarly, several countries and regions, including the Netherlands, Australia, France, and United States, have implemented wastewater surveillance programs to monitor for SARS-CoV-2 and other pathogens (*17*–*18*), providing timely data on disease prevalence and transmission dynamics. In addition, specific early warning components such as the European Antimicrobial Resistance Surveillance Network (EARS-Net) (*19*), prescription surveillance in Japan (*20*), and the Over-The-Counter (OTC) medication sales monitoring in the United States provide parallel data streams that are synergistically integrated into broader surveillance frameworks (*21*). The EARS-Net tracks antimicrobial resistance patterns as part of the European disease and laboratory networks. Meanwhile, OTC medication sales monitoring and prescription surveillance analyze sales data for specific drugs as an

TABLE 1. Major indicator-based surveillance systems.

System (website)	Country/ region (year started)	Data sources	Data access	Functions	Features
NIDRIS (*1*)	China (2004)	Medical institutions	Restricted	The healthcare departments review infectious disease information reported by medical institutions and then report to NIDRIS. It monitors individual cases, diagnoses, and epidemiological information on 39 infectious diseases.	Case surveillance. Multisectoral cooperation.
NNDSS (https://www.cdc.gov/nndss/index.html) (*9*)	United States (Before 1990)	Health departments, healthcare providers, laboratories, and hospitals	Public	The health departments work with healthcare providers, laboratories, hospitals, and other partners to obtain information. Surveillance of notifiable disease cases was carried out in about 3,000 health institutions.	Case surveillance. Multi-source data and multisectoral cooperation.
TESSy (https://www.ecdc.europa.eu/en/publications-data/european-surveillance-system-tessy) (*10*)	Europe (2008)	European Union member states	Restricted	Surveillance of notifiable infectious disease cases.	Case surveillance. International cooperation.
CIDARS (*1*)	China (2008)	Data reported in NIDRIS	Restricted	Case data extraction, early warning analysis, and signal push daily. It analyzes the situation of 39 infectious diseases and provides early warning to provincial and municipal CDCs.	Case surveillance
ELR (https://www.cdc.gov/elr/index.html) (*11*)	United States (2001)	Laboratories	Restricted	ELRs are transmitted from the laboratory to public health departments, health care systems, and CDCs for further public health action. It monitors laboratory testing information.	Laboratory surveillance. Multisectoral cooperation.
IASR (https://www.niid.go.jp/niid/ja/iasr.html)	Japan (1980)	Local public health laboratories, public health centers, and quarantine stations throughout the country.	Public	Surveillance of laboratory testing information, including pathogen differential diagnosis, genetic testing, and drug resistance test results.	Laboratory surveillance. Multi-source data and multisectoral cooperation.
NSSP (https://www.cdc.gov/nssp/php/about/index.html) (*14*)	United States (2003)	Emergency department, laboratories, medical centers, weather service data	Restricted	By tracking the symptoms of patients in the emergency department and other environments in almost real-time, a timely system is provided for public health officials to detect, understand, and monitor health threats to determine whether they need to be addressed.	Syndromic surveillance. Multi-source data and multisectoral cooperation.
EARS-Net (https://www.ecdc.europa.eu/en/about-us/networks/disease-networks-and-laboratory-networks/ears-net-data) (*19*)	Europe (1998)	National antimicrobial resistance surveillance initiatives, laboratory networks	Public	Collect comparable, representative, and accurate data on antimicrobial resistance, analyze the spatiotemporal trends of antimicrobial resistance in Europe, and provide support for policy decision-making	Laboratory surveillance. International cooperation.
Prescription surveillance (*20*)	Japan (2009)	Pharmacies	Restricted	Report the estimated numbers of influenza and varicella patients and people prescribed certain drugs.	Surveillance of drug purchases.

Abbreviation: NIDRIS=National Notifiable Infectious Diseases Reporting Information System; NNDSS=National Notifiable Diseases Surveillance System; TESSy=The European Surveillance System; CIDARS=China Infectious Diseases Automated-Alert and Response System; ELR=Electronic Laboratory Reporting system; IASR=Infectious Agents Surveillance Report; NSSP=National Syndromic Surveillance Program; EARS-Net=European Antimicrobial Resistance Surveillance Network.

important component of syndromic surveillance to identify trends that may indicate disease transmission. Most of these systems involve multisectoral collaboration for data validation or further public health action.

Indicator-based surveillance systems are characterized by their specificity, as they rely on physician-diagnosed and laboratory-confirmed data, utilizing pre-defined case definitions and/or laboratory testing to ensure a clear and consistent identification of cases. Typically, indicator-based surveillance reports are compiled on a weekly or monthly basis from primary

public health units, which ensures a more complete and specific dataset, albeit at the cost of timeliness. This reporting frequency may lead to reporting delays and information omissions, which in turn can result in lagging or missed warnings, particularly for emerging infectious diseases where the case definitions may not yet be well-established or the disease may present with atypical symptoms.

Event-Based Surveillance Systems

The prevalent event-based surveillance systems are primarily web-based, capturing all unstructured data that appears on the internet, including social media posts, search inquiries, e-commerce trends, and wearable device records (*22*). Event-based surveillance systems can be further categorized into news aggregators, automatic and moderated systems (*7*–*8*). News aggregators aggregate web content by location or topic into one platform for convenient access, such as Influenzanet (*23*), FluTracking (*24*), and Google Flu Trends (*25*), the last of which is no longer updated. Automatic systems add a series of analytic steps to news aggregators, as seen in the Semantic Processing and Integration of Distributed Electronic Resources for Epidemiology (EpiSPIDER) (*26*), HealthMap (*27*), BioCaster (*28*), EPIWATCH (*29*), and the Medical Information System (MedISys) (*30*). Moderated systems involve the screening of information by public health professionals before reports release, thus exhibiting fewer false positives compared to news aggregators and automatic systems, exemplified by GPHIN (*31*), ProMED-mail (*32*), and Argus (*33*). A summary of the characteristics of the ten event-based surveillance systems is presented in Table 2.

Web-based surveillance systems commonly use multilingual and multi-source data to monitor vast amounts of online information on infectious diseases. For instance, HealthMap, an automatic system operational since 2006, monitors online information on emerging diseases in nine languages, utilizing data from sources like Baidu, EuroSurveillance, Google, and WHO, among others (*27*). MedISys, operating within the European Union since 2004, collects public health reports in 32 languages from global internet sources, providing summaries on various diseases (*30*). Argus, a moderated system, collects information from media sources in 40 native languages and uses Bayesian analysis tools for filtering and selection, focusing on biological events posing global health threats (*33*). Some systems use advanced AI technology to drive data analysis. For example, BioCaster, relaunched in 2021, utilizes deep learning and natural language processing models to analyze structurally complex data from thousands of news reports daily, enabling real-time detection and interactive visualization of outbreak reports (*34*). EPIWATCH employs AI to scan open-source data, detecting early warnings of infectious disease outbreaks since 2016, with continuous enhancements through machine learning (*29*). GPHIN implements a machine learning classifier to score the relevance of reports, distinguishing outbreak-related stories from background noise, with high-scoring articles published immediately and low-scoring ones suppressed, while medium-relevance articles are reviewed by analysts (*35*). The integration of advanced technologies enables these systems to demonstrate significant advantages in capturing early abnormal signals, thereby facilitating the timely detection and management of public health threats. Influenzanet and FluTracking are two representative participatory surveillance platforms that collect data from volunteers at multiple stages of symptoms, absence from school or work, medication, medical consultations, and vaccinations. Participatory surveillance improves previous health surveillance systems by involving the public in the construction of epidemiologic scenarios (*36*–*37*).

Event-based surveillance systems enable timely surveillance and early warning by facilitating immediate reporting and rapid investigation of diseases of public health significance. Event-based surveillance serves as a complementary early warning mechanism for emerging infectious diseases, emphasizing the importance of immediate reporting and management to ensure a swift response, which is also an essential feature that distinguishes it from indicator-based surveillance. For example, GPHIN has been recognized for its role in detecting early signals during public health emergencies, such as the SARS outbreak in 2003 and the initial reports of the Ebola outbreak in West Africa in 2014 (*38*). It is worth noting that GPHIN's contributions are part of a broader array of surveillance and intelligence efforts, whose alerts are based on a combination of local accounts and media reports that collectively contribute to the early identification of potential outbreaks. However, the information obtained by event-based surveillance systems is not fully verified by public health professionals, so the reliability of the information they monitor cannot be guaranteed. When used for early warning, their low signal-to-noise ratio might drain considerable public health resources (*5*). Hence,

TABLE 2. Major event-based surveillance systems.

System (website)	Type	Country/ region (year started)	Area of Service	Data sources	Data access	Functions	Features
HealthMap (https://healthmap.org/about/) (*27*)	Automatic system	United States (2006)	Worldwide	Baidu, EuroSurveillance, Google, HealthMap Community News Reports, WOAH, ProMED, User Eyewitness Reports, and WHO	Public	Online information on emerging diseases is monitored in nine languages, providing real-time surveillance of public health threats based on informal data sources	Multi-source data and multilanguage
EpiSPIDER (http://www.epispider.org/) (*26*)	Automatic system	United States (2006)	North America, Europe, Australia, Asia	Daylife, Google, Humanitarian News, Moreover, ProMED, Twitter, and WHO	Public	Integrate information collected from online media and informal surveillance systems in English to monitor outbreaks of infectious diseases	Multi-source data
MedISys (http://medusa.jrc.it) (*30*)	Automatic system	Europe (2004)	European Union	Global internet resources	Restricted /Limited to European Union member states	Collect public health reports in 32 languages from global internet sources and compile summaries of information on various diseases	Multi-source data and multilanguage
Argus (*33*)	Moderated system	United States (2004)	Worldwide	Printed newspapers, electronic media, Internet-based newsletters and blogs, WHO, and WOAH	Restricted	Information is collected from media sources in 40 native languages, and Bayesian analysis tools are used to select and filter the information. It aims to monitor biological events that may pose a global health threat to humans, plants and animals	Multi-source data and multilanguage
ProMED-mail (https://promedmail.org/) (*32*)	Moderated system	United States (1994)	Worldwide	Media reports, official reports, online summaries, and local observers	Public	A transparent, non-political, open to all, free e-mail list for identifying emerging and re-emerging infectious diseases and unusual health toxin-related events	Multi-source data and multilanguage
BioCaster (http://biocaster.nii.ac.jp) (*34*)	Automatic system	Japan (2006)	Priority to Asia-Pacific region	EurekAlert!, European Media Monitor Alerts, Google, the CDC's Morbidity and Mortality Weekly Report, MeltWater, WOAH, ProMED, Reuters, WHO and Vetsweb	Public	An ontology-based text mining system that detects and tracks the distribution of infectious diseases from the internet in eight languages. A quantum leap in real-time detection of disease outbreaks has been achieved through the integration of artificial intelligence technology	Multi-source data, multilanguage, and advanced technology
EPIWATCH (https://www.epiwatch.org/) (*29*)	Automatic system	Australia (2016)	Worldwide	Media coverage, press releases, official reports, and social media	Public	An open-source epidemic observation station based on artificial intelligence that searches global internet resources in 52 languages to promptly detect infectious disease outbreaks. The system is enhanced by the integration of artificial intelligence and machine learning technologies	Multi-source data, multilanguage, and advanced technology
GPHIN (https://gphin.canada.ca/) (*31*)	Moderated system	Canada (1997)	Worldwide	News service items, ProMED-mail, electronic discussion groups, and selected websites	Restricted /Subscription	Surveillance of global media messages in nine languages to detect and track major public health events and provide real-time, early warning based on the international internet sources. The latest generation of GPHIN integrates machine learning technology (*35*)	Multi-source data, multilanguage, and advanced technology

Continued

System (website)	Type	Country/ region (year started)	Area of Service	Data sources	Data access	Functions	Features
Influenzanet (https://influenzanet.info/explore-data) (*23*)	News aggregator	Europe (2003)	The Netherlands, Belgium, Portugal, Italy, the UK, France, Sweden, Spain, Ireland, Denmark, and Switzerland	Online survey	Public	Influenza-like illness (ILI) incidence in Europe was monitored by screening the ILI questionnaire completed by volunteers. In the questionnaire, participants are asked to report information on symptoms, date of onset, absence from school or work, medication, and medical consultations and outcomes	Participatory surveillance and multi-stage surveillance
FluTracking (https://info.flutracking.net/) (*24*)	News aggregator	Australia (2006)	Australia	Online survey	Public	A participatory surveillance system to monitor the spread and severity of ILI in Australia by investigating symptoms (cough, fever, and sore throat), time off work or normal duties, influenza vaccination status, influenza laboratory testing, and health-seeking behaviors	Participatory surveillance and multi-stage surveillance

Abbreviation: WOAH=World Organization for Animal Health; ProMED=Program for Monitoring Emerging Diseases; WHO=World Health Organization; EpiSPIDER=Semantic Processing and Integration of Distributed Electronic Resources for Epidemiology; MedISys=Medical Information System; GPHIN=Global Public Health Intelligence Network

improving data quality from event-based surveillance should be an ongoing endeavor.

Commonalities Between Surveillance Systems

Concerning data collection, first, the data are multi-sourced. Although surveillance data were initially derived from clinical diagnoses and laboratory tests, with the emergence and use of big data technology, the data sources have expanded to include symptoms, human behavior, and social activities, which have diversified the types of data available for infectious disease surveillance. Second, information sharing has been enhanced through transnational cooperation, which enables faster responses to infectious disease threats by fostering collaboration among international organizations, government agencies, and non-governmental organizations, and through multidisciplinary collaboration, in which experts from various fields work together to advance infectious disease surveillance systems.

At the data analysis stage, modern surveillance systems have embraced a range of sophisticated methodologies to systematically process and interpret the vast and diverse datasets they collect. These methods include high-throughput analysis, which allows for the rapid examination of large volumes of data (*39*); aberration detection techniques, such as control charts and linear regressions, which identify deviations from expected patterns that may indicate the onset of an outbreak (*40*); and spatiotemporal clustering algorithms, which help in pinpointing the geographic and temporal distributions of cases (*41*). For example, the CDC in the United States uses the Early Aberration Reporting System to detect anomalies in disease surveillance data (*42*). Likewise, public health institutes in European countries use the Farrington algorithm, a quasi-Poisson regression model, to monitor disease incidence across member states (*43*). These traditional methods remain foundational in public health surveillance, but there has been a notable increase in the adoption of more sophisticated techniques, such as machine learning and Bayesian frameworks, particularly for multivariate datasets. For example, EPIWATCH's ability to provide early outbreak signals has been enhanced by AI and machine learning (*29*). Moreover, AI can be used to develop predictive models that can forecast the spread of infectious diseases based on various factors, including environmental conditions, population movements, and historical outbreak data. These algorithms learn from patterns and trends in the data, improving their accuracy over time and providing valuable insights that complement traditional surveillance data.

In terms of outputs, early warning sensitivity and accuracy are constantly improving. Systems based on online media can serve as a valuable complement to

official surveillance and early warning systems, offering more timely warnings and improved sensitivity. Moreover, despite the heterogeneous nature of internet surveillance information, technological advances can significantly reduce data noise, and thus, the accuracy of early warning is also rising. This evolution ensures that public health responses are increasingly informed by precise and timely data, enabling a more effective containment of infectious disease threats.

DISCUSSION AND FUTURE DIRECTIONS

International experience in constructing infectious disease surveillance systems has provided beneficial insights for China. The NIDRIS and CIDARS systems currently used in China are based on analyses of clinically confirmed cases. Although highly accurate, this approach often results in a significant lag. Surveillance and early warning platforms can be established at multiple stages before the diagnosis of infectious disease patients, including risk factors, symptoms, medication purchases, absenteeism from work or school, and medical consultations. In this case, warning signals can be released earlier, which is critical for the early management of infectious diseases (*2*). Some syndromic surveillance systems have been established in China, but they only operate on a pilot basis in certain regions (*44*–*45*). Establishing participatory syndromic surveillance systems at the national level could enhance surveillance activities. For example, collecting crowdsourced data on influenza-like illnesses to track respiratory viruses promptly. Event-based internet surveillance systems complement NIDRIS and CIDARS by highlighting potentially contagious cases that have not been clinically confirmed. Carefully screening and integrating valid information can better address potential risks. Recent scientific recommendations, such as the 7-1-7 metric, have been proposed to quantify outbreak surveillance, notification, and response performance. The 7-1-7 framework measures the timeliness of surveillance (target of ≤7 days from emergence), notification (target of ≤1 day from detection), and completion of seven early response activities (target of ≤7 days from notification) (*46*). Implementing such metrics may help identify bottlenecks and enablers within the system, thereby facilitating targeted improvements and prioritizing national planning for early outbreak management.

Second, NIDRIS and CIDARS primarily collect data from healthcare institutions, and data exchange between different sectors is limited. It is necessary to consider utilizing data from sources such as media, schools, workplaces, pharmacies, laboratories, and customs. Enhanced multisectoral cooperation and information-sharing are crucial for obtaining comprehensive information on disease and health-related events (*2*). Furthermore, China should exchange information on infectious diseases with other countries. The WHO established a new global hub for pandemic and epidemic intelligence in Berlin, Germany (*47*), to enhance data sharing and international cooperation for the early detection of potential pandemics. This hub, in collaboration with the EIOS initiative, supports a unified, all-hazards, One Health approach to the early detection, verification, assessment, and communication of public health threats using publicly available information (*48*). EIOS facilitates global, multisectoral collaboration, supporting countries and other stakeholders in addressing future pandemic and epidemic risks with improved access to data, enhanced analytical capacities, and improved tools and insights for decision-making. China should, as always, actively participate in global infectious disease early warning efforts, leveraging initiatives like EIOS to strengthen its contribution to global health security.

Finally, the early warning model of China's infectious disease surveillance platform, represented by CIDARS, is primarily based on the fixed-threshold detection method, temporal models, and spatial-temporal models (*49*). As technology advances, CIDARS should be updated to enhance its data integration and intelligent learning abilities to improve the effectiveness of early warnings (*2*). Modern, intelligent surveillance systems require AI algorithms to rapidly collect, efficiently process, and thoroughly analyze large-scale, multi-source data for timely and accurate outbreak warnings. Additionally, diverse data formats, including text, images, video, and audio, may necessitate the use of blockchain and multimodal technologies to consolidate them into a structured database, enabling collaborative management of heterogeneous data from various sources. However, the successful implementation of AI in surveillance systems also requires a skilled workforce with expertise in epidemiology, advanced data analysis, and system management. In China, a notable shortage of CDC professionals limits the improvement of infectious disease surveillance, management, and emergency

response capabilities. Therefore, targeted training of professionals who can interpret AI outputs, conduct epidemiological investigations, and make informed decisions based on complex data is essential. On October 25, 2023, China established the National Data Bureau to coordinate data integration and promote the development of a digital China. The Bureau will accelerate digital technology innovations and assist in building intelligent surveillance systems while fostering the development of a highly skilled public health workforce to ensure the effective utilization of these advanced technologies.

The China CDC leadership has steadily strengthened the surveillance and early warning capacity of provincial CDCs. Intelligent, multipoint-triggered early warning models are being explored in several PLADs. Decentralizing early warning tasks to PLADs is a crucial strategic innovation that allows customization to regional factors, facilitating accurate monitoring and resource deployment. This decentralization is imperative because it enables efficient and timely detection, verification, investigation, and early response at a more localized level, further enhancing the national surveillance system's overall efficiency. However, differences in surveillance capacity among provincial CDCs may compromise the accuracy and comparability of results. Moreover, competition among provincial CDCs may hinder infectious disease data sharing, as infectious disease surveillance and early warning are linked to CDC performance evaluations. Therefore, information-sharing mechanisms across PLADs are needed to ensure accurate and complete data for timely infectious disease prevention.

The numerous practical challenges in constructing intelligent, multipoint-triggered surveillance systems must be recognized. For example, multi-point surveillance collects large quantities of user data, which inevitably carries the risk of leaking private information. Thus, technologies like decentralization and data encryption are necessary for privacy protection. Furthermore, a key challenge with event-based surveillance is distinguishing between true and false information. Therefore, information filtering and verification strategies are needed to determine the credibility of surveillance data.

CONCLUSION

In summary, China's current infectious disease surveillance systems should be upgraded to meet new-era requirements. According to the findings of this review, the term "multipoint-triggered" implies multi-source data, multi-stage monitoring, and multisectoral and multi-provincial cooperation. The term "intelligent" implies the application of advanced and learning-capable warning models and analysis techniques. Intelligent and multipoint-triggered infectious disease surveillance systems will significantly improve the timeliness and accuracy of early warnings and further strengthen China's ability to respond to public health emergencies.

Conflicts of interest: No conflicts of interest.

Funding: Supported by the National Natural Science Foundation of China (82204162, 81973150). Professor Yuantao Hao gratefully acknowledges the support of K.C.Wong Education Foundation.

doi: 10.46234/ccdcw2024.220

[#] Corresponding author: Yuantao Hao, haoyt@bjmu.edu.cn.

[1] Department of Epidemiology and Biostatistics, School of Public Health, Peking University, Beijing, China; [2] Peking University Center for Public Health and Epidemic Preparedness & Response, Beijing, China; [3] Key Laboratory of Epidemiology of Major Diseases (Peking University), Ministry of Education, Beijing, China.

Submitted: November 23, 2023; Accepted: July 09, 2024

REFERENCES

1. Yang WZ, Li ZJ, Lan YJ, Wang JF, Ma JQ, Jin LM, et al. A nationwide web-based automated system for outbreak early detection and rapid response in China. Western Pac Surveill Response J 2011;2(1):10 – 5. https://doi.org/10.5365/WPSAR.2010.1.1.009.
2. Yang WZ, Lan YJ, Lyu W, Leng ZW, Feng LZ, Lai SJ, et al. Establishment of multi-point trigger and multi-channel surveillance mechanism for intelligent early warning of infectious diseases in China. Chin J Epidemiol 2020;41(11):1753 – 7. https://doi.org/10.3760/cma.j.cn112338-20200722-00972.
3. Wang LP, Jin LM, Xiong WY, Tu WX, Ye CC. Chapter 2 - Infectious disease surveillance in China. In: Yang WZ, editor. Early warning for infectious disease outbreak: theory and practice. London: Academic Press. 2017; p. 23-33. http://dx.doi.org/10.1016/B978-0-12-812343-0.00002-3.
4. Thurmond MC. Conceptual foundations for infectious disease surveillance. J Vet Diagn Invest 2003;15(6):501 – 14. https://doi.org/10.1177/104063870301500601.
5. Huang S, Liu CX, Deng Y, Zhang CH, Fan SM, Zheng JD, et al. Progress in the practice of surveillance and early warning of infectious diseases in major countries and regions. Chin J Epidemiol 2022;43(4):591 – 7. https://doi.org/10.3760/cma.j.cn112338-20211105-00856.
6. Paquet C, Coulombier D, Kaiser R, Ciotti M. Epidemic intelligence: a new framework for strengthening disease surveillance in Europe. Euro Surveill 2006;11(12):212-4. https://pubmed.ncbi.nlm.nih.gov/17370970/.
7. O'Shea J. Digital disease detection: a systematic review of event-based internet biosurveillance systems. Int J Med Inform 2017;101:15 – 22. https://doi.org/10.1016/j.ijmedinf.2017.01.019.
8. Choi J, Cho Y, Shim E, Woo H. Web-based infectious disease surveillance systems and public health perspectives: a systematic review. BMC Public Health 2016;16(1):1238. https://doi.org/10.1186/s12889-

016-3893-0.
9. Centers for Disease Control and Prevention (CDC). Demographic differences in notifiable infectious disease morbidity--United States, 1992-1994. MMWR Morb Mortal Wkly Rep 1997;46(28):637-41. https://www.cdc.gov/mmwr/preview/mmwrhtml/00048395.htm.
10. Ammon A, Faensen D. Surveillance of infectious diseases at the EU level. Bundesgesundheitsblatt Gesundheitsforschung Gesundheitsschutz 2009;52(2):176 – 82. https://doi.org/10.1007/s00103-009-0759-y.
11. Gluskin RT, Mavinkurve M, Varma JK. Government leadership in addressing public health priorities: strides and delays in electronic laboratory reporting in the United States. Am J Public Health 2014;104 (3):e16 – 21. https://doi.org/10.2105/AJPH.2013.301753.
12. Jayatilleke A, Kriseman J, Bastin LH, Ajani U, Hicks P. Syndromic surveillance in an ICD-10 world. AMIA Annu Symp Proc 2014;2014: 1806-14. https://pubmed.ncbi.nlm.nih.gov/25954453/.
13. Thomas MJ, Yoon PW, Collins JM, Davidson AJ, Mac Kenzie WR. Evaluation of syndromic surveillance systems in 6 US state and local health departments. J Public Health Manag Pract 2018;24(3):235 – 40. https://doi.org/10.1097/PHH.0000000000000679.
14. Centers for Disease Control and Prevention. National syndromic surveillance program (NSSP). 2024. https://www.cdc.gov/nssp/php/about/index.html. [2024-7-3].
15. Smith GE, Elliot AJ, Lake I, Edeghere O, Morbey R, Catchpole M, et al. Syndromic surveillance: two decades experience of sustainable systems - its people not just data! Epidemiol Infect 2019;147:e101. http://dx.doi.org/10.1017/S0950268819000074.
16. Klapsa D, Wilton T, Zealand A, Bujaki E, Saxentoff E, Troman C, et al. Sustained detection of type 2 poliovirus in London sewage between February and July, 2022, by enhanced environmental surveillance. Lancet 2022;400(10362):1531 – 8. https://doi.org/10.1016/S0140-6736(22)01804-9.
17. Kitajima M, Ahmed W, Bibby K, Carducci A, Gerba CP, Hamilton KA, et al. SARS-CoV-2 in wastewater: state of the knowledge and research needs. Sci Total Environ 2020;739:139076. https://doi.org/10.1016/j.scitotenv.2020.139076.
18. Izquierdo-Lara RW, Heijnen L, Oude Munnink BB, Schapendonk CME, Elsinga G, Langeveld J, et al. Rise and fall of SARS-CoV-2 variants in Rotterdam: comparison of wastewater and clinical surveillance. Sci Total Environ 2023;873:162209. https://doi.org/10.1016/j.scitotenv.2023.162209.
19. European Centre for Disease Prevention and Control. European antimicrobial resistance surveillance network (EARS-Net). 2023. https://www.ecdc.europa.eu/en/about-us/networks/disease-networks-and-laboratory-networks/ears-net-data. [2024-7-3].
20. Sugawara T, Ohkusa Y, Kawanohara H, Kamei M. Prescription surveillance for early detection system of emerging and reemerging infectious disease outbreaks. Biosci Trends 2018;12(5):523 – 5. https://doi.org/10.5582/bst.2018.01201.
21. Das D, Metzger K, Heffernan R, Balter S, Weiss D, Mostashari F, et al. Monitoring over-the-counter medication sales for early detection of disease outbreaks--New York City. MMWR Suppl 2005;54:41-6. https://pubmed.ncbi.nlm.nih.gov/16177692/.
22. Ouyang LW, Yuan Y, Cao YM, Wang FY. A novel framework of collaborative early warning for COVID-19 based on blockchain and smart contracts. Inf Sci 2021;570:124 – 43. https://doi.org/10.1016/j.ins.2021.04.021.
23. Koppeschaar CE, Colizza V, Guerrisi C, Turbelin C, Duggan J, Edmunds WJ, et al. Influenzanet: citizens among 10 countries collaborating to monitor influenza in Europe. JMIR Public Health Surveill 2017;3(3):e66. https://doi.org/10.2196/publichealth.7429.
24. Dalton C, Carlson S, Butler M, Cassano D, Clarke S, Fejsa J, et al. Insights from flutracking: thirteen tips to growing a web-based participatory surveillance system. JMIR Public Health Surveill 2017;3 (3):e48. https://doi.org/10.2196/publichealth.7333.
25. Kandula S, Shaman J. Reappraising the utility of Google Flu Trends. PLoS Comput Biol 2019;15(8):e1007258. https://doi.org/10.1371/journal.pcbi.1007258.
26. Lyon A, Nunn M, Grossel G, Burgman M. Comparison of web-based biosecurity intelligence systems: BioCaster, EpiSPIDER and HealthMap. Transbound Emerg Dis 2012;59(3):223 – 32. https://doi.org/10.1111/j.1865-1682.2011.01258.x.
27. Madoff LC, Li A. Web-based surveillance systems for human, animal, and plant diseases [J]. Microbiol Spectr, 2014; 2 (1), 10. DOI: 10.1128/microbiolspec.oh-0015-2012.
28. Collier N, Doan S, Kawazoe A, Goodwin RM, Conway M, Tateno Y, et al. BioCaster: detecting public health rumors with a Web-based text mining system. Bioinformatics 2008;24(24):2940 – 1. https://doi.org/10.1093/bioinformatics/btn534.
29. Hutchinson D, Kunasekaran M, Quigley A, Moa A, MacIntyre CR. Could it be monkeypox? Use of an AI-based epidemic early warning system to monitor rash and fever illness. Public Health 2023;220:142 – 7. https://doi.org/10.1016/j.puhe.2023.05.010.
30. Linge JP, Steinberger R, Fuart F, Bucci S, Belyaeva J, Gemo M, et al. MedISys: medical information system. In: Asimakopoulou E, Bessis N, editors. Advanced ICTs for disaster management and threat detection: collaborative and distributed frameworks. Hershey, PA, USA: IGI Global. 2010; p. 131-42. http://dx.doi.org/10.4018/978-1-61520-987-3.ch009.
31. Mykhalovskiy E, Weir L. The Global Public Health Intelligence Network and early warning outbreak detection: a Canadian contribution to global public health. Can J Public Health 2006;97(1): 42 – 4. https://doi.org/10.1007/BF03405213.
32. Carrion M, Madoff LC. ProMED-mail: 22 years of digital surveillance of emerging infectious diseases. Int Health 2017;9(3):177 – 83. https://doi.org/10.1093/inthealth/ihx014.
33. Chen HC, Zeng D, Yan P. Argus. In: Chen HC, Zeng D, Yan P, editors. Infectious disease informatics: syndromic surveillance for public health and bio-defense. New York, NY: Springer. 2010; p. 177-81. http://dx.doi.org/10.1007/978-1-4419-1278-7_13.
34. Meng ZQ, Okhmatovskaia A, Polleri M, Shen YN, Powell G, Fu ZH, et al. BioCaster in 2021: automatic disease outbreaks detection from global news media. Bioinformatics 2022;38(18):4446 – 8. https://doi.org/10.1093/bioinformatics/btac497.
35. Carter D, Stojanovic M, Hachey P, Fournier K, Rodier S, Wang YL, et al. Global public health surveillance using media reports: redesigning GPHIN. Stud Health Technol Inform 2020;270:843 – 7. https://doi.org/10.3233/SHTI200280.
36. Guerrisi C, Turbelin C, Souty C, Poletto C, Blanchon T, Hanslik T, et al. The potential value of crowdsourced surveillance systems in supplementing sentinel influenza networks: the case of France. Euro Surveill 2018;23(25):1700337. https://doi.org/10.2807/1560-7917.ES.2018.23.25.1700337.
37. Leal Neto O, Cruz O, Albuquerque J, de Sousa MN, Smolinski M, Pessoa Cesse EÂ, et al. Participatory surveillance based on crowdsourcing during the Rio 2016 Olympic games using the guardians of health platform: descriptive study. JMIR Public Health Surveill 2020;6(2):e16119. https://doi.org/10.2196/16119.
38. Dion M, AbdelMalik P, Mawudeku A. Big data and the global public health intelligence network (GPHIN). Can Commun Dis Rep 2015;41 (9):209 – 14. https://doi.org/10.14745/ccdr.v41i09a02.
39. den Hartog G, van Binnendijk R, Buisman AM, Berbers GAM, van der Klis FRM. Immune surveillance for vaccine-preventable diseases. Expert Rev Vaccines 2020;19(4):327 – 39. https://doi.org/10.1080/14760584.2020.1745071.
40. Yuan MR, Boston-Fisher N, Luo Y, Verma A, Buckeridge DL. A systematic review of aberration detection algorithms used in public health surveillance. J Biomed Inform 2019;94:103181. https://doi.org/10.1016/j.jbi.2019.103181.
41. Lan Y, Delmelle E. Space-time cluster detection techniques for infectious diseases: a systematic review. Spat Spatiotemporal Epidemiol 2023;44:100563. https://doi.org/10.1016/j.sste.2022.100563.
42. Tokars JI, Burkom H, Xing J, English R, Bloom S, Cox K, et al. Enhancing time-series detection algorithms for automated biosurveillance. Emerg Infect Dis 2009;15(4):533 – 9. https://doi.org/10.3201/1504.080616.
43. Hulth A, Andrews N, Ethelberg S, Dreesman J, Faensen D, van Pelt W,

et al. Practical usage of computer-supported outbreak detection in five European countries. Euro Surveill 2010;15(36):19658. https://pubmed.ncbi.nlm.nih.gov/20843470/.
44. Ye CC, Li ZJ, Fu YF, Lan YJ, Zhu WP, Zhou DL, et al. SCM: a practical tool to implement hospital-based syndromic surveillance. BMC Res Notes 2016;9:315. https://doi.org/10.1186/s13104-016-2098-z.
45. Yan WR, Palm L, Lu X, Nie SF, Xu B, Zhao Q, et al. ISS-an electronic syndromic surveillance system for infectious disease in rural China. PLoS One 2013;8(4):e62749. https://doi.org/10.1371/journal.pone.0062749.
46. Bochner AF, Makumbi I, Aderinola O, Abayneh A, Jetoh R, Yemanaberhan RL, et al. Implementation of the 7-1-7 target for detection, notification, and response to public health threats in five countries: a retrospective, observational study. Lancet Glob Health 2023;11(6):e871 – 9. https://doi.org/10.1016/S2214-109X(23)00133-X.
47. World Health Organization. WHO, Germany launch new global hub for pandemic and epidemic intelligence. 2021. https://www.who.int/news/item/05-05-2021-who-germany-launch-new-global-hub-for-pandemic-and-epidemic-intelligence. [2023-10-30].
48. World Health Organization. Epidemic intelligence from open sources. 2022. https://www.who.int/initiatives/eios. [2024-7-3].
49. Yang WZ, Li ZJ, Lan YJ, Ma JQ, Jin LM, Lai SJ, et al. Chapter 7 - China infectious diseases automated-alert and response system (CIDARS). In: Yang WZ, editor. Early warning for infectious disease outbreak: theory and practice. London: Academic Press. 2017; p. 133-61. https://doi.org/10.1016/B978-0-12-812343-0.00007-2.

Youth Editorial Board

Indexed by Science Citation Index Expanded (SCIE), Social Sciences Citation Index (SSCI), PubMed Central (PMC), Scopus, Chinese Scientific and Technical Papers and Citations, and Chinese Science Citation Database (CSCD)

The inauguration of *China CDC Weekly* is in part supported by Project for Enhancing International Impact of China STM Journals Category D (PIIJ2-D-04-(2018)) of China Association for Science and Technology (CAST).

CCDC weekly

Vol. 6 No. 41 Oct. 11, 2024

Responsible Authority
National Disease Control and Prevention Administration

Sponsor
Chinese Center for Disease Control and Prevention

Editing and Publishing
China CDC Weekly Editorial Office
No.155 Changbai Road, Changping District, Beijing, China
Tel: 86-10-63150501, 63150701
Email: weekly@chinacdc.cn

CSSN
ISSN 2096-7071 (Print)
ISSN 2096-3101 (Online)
CN 10-1629/R1